DEUTSCHES ELEKTRONEN – SYNCHROTRON

DESY 92–058
April 1992

Rare B-Decays in QCD

A. Ali

Deutsches Elektronen-Synchrotron DESY, Hamburg

ISSN 0418-9833

NOTKESTRASSE 85 · D-2000 HAMBURG 52

To be sure that your preprints are promptly included in the
HIGH ENERGY PHYSICS INDEX,
send them to (if possible by air mail):

DESY Bibliothek Notkestraße 85 W-2000 Hamburg 52 Germany	DESY-IfH Bibliothek Platanenallee 6 O-1615 Zeuthen Germany

DESY 92-058
April 1992

ISSN 0418-9833

Rare B-Decays in QCD

Ahmed Ali

Deutsches Elektronen Synchrotron - DESY
Hamburg, Germany

Abstract

We review theoretical work done on rare B-decays in the context of the Standard Model (SM) of electroweak interactions. The framework used is that of QCD, which is applied to calculate the decay rates and distributions in a number of processes, such as $B \to X_s + \gamma$, $B \to X_d + \gamma$, $B \to X_s + \ell^+\ell^-$, and $B \to X_s + \nu\bar{\nu}$, where X_s and X_d denote light hadrons with an overall quantum number $S = -1$ and $S = 0$, respectively. We particularly emphasize inclusive measurements in this sector, which would eventually permit a more reliable comparison of the SM predictions and experiments. However, we also discuss estimates of some exclusive rare B-decay modes, calculated in the vector meson dominance approximation and using the heavy quark effective theory (HQET). The importance of measuring the CKM-suppressed rare B-decays in determining the CKM matrix-element V_{td} is underlined. Rate estimates in some inclusive and exclusive suppressed rare decay modes are presented by imposing current experimental constraints on the CKM matrix.

*To be published in the Proceedings of the 1991 ICTP, Trieste, Summer School in High Energy Physics and Cosmology, World Scientific Publishers, Singapore (1992).

Contents

1 INTRODUCTION

B-physics is now nearly two decades old. In the Standard Model of electroweak interactions (SM) [1], the existence of the third generation of fermions was postulated by Kobayashi and Maskawa [2] in 1973 to admit the phenomenon of CP-violation. The resulting (3×3) matrix in the flavour space, which is a generalization of the Cabibbo-GIM matrix [3,4], has a non-trivial phase. The determination of the matrix-elements of this (aptly called the Cabibbo-Kobayashi-Maskawa (CKM)) matrix is the main aim of experiments and theory in flavour physics. Experimental B-physics was initiated in 1977 with the discovery of the Υ-resonances by the Columbia-Fermilab-Stony Brook collaboration (CSF), led by Lederman [5,6,7]. The Fermilab discoveries of the first three resonances, $\Upsilon(9.5\ GeV), \Upsilon'(10.0\ GeV)$ and $\Upsilon''(10.4\ GeV)$, were subsequently confirmed by experiments in e^+e^- annihilation at the energy upgraded DORIS [8,9,10] and later at CESR [11,12], which also established the quantum numbers $J^{PC} = 1^{--}$ and the $(b\bar{b})$ bound state nature of these resonances. Since these pioneering experiments, spectroscopy of the $(b\bar{b})$ system has come a long way with the discovery of many more states having the quantum numbers $1^{--}, 0^{++}, 1^{++}$ and 2^{++}. In the meanwhile the nomenclature of these states has changed; they are now characterized by their radial and orbital angular momentum quantum numbers and spin $(n\ ^{2s+1}L_J)$ with $L = S, P, D, ...$ in accordance with the atomic physics convention [13]. Of the $(n\ ^3S_1)$ states, $\Upsilon(4S)$ and higher resonances lie above the $B\bar{B}$-threshold. The decay $\Upsilon(4S) \to B\bar{B}$ is, in fact, the best source of information on the properties of B-hadrons, with the ARGUS and CLEO collaborations being the principal experimental groups involved in these studies. In addition, valuable contribution to B-physics has been made by experiments in high energy e^+e^- machines, PETRA, PEP, KEK, LEP, and SLC, and in $p\bar{p}$ collisions at CERN and Fermilab. We refer to a recent volume on B-decays for a detailed account of the history of B-physics and its up to date status [14].

The main topic of these lectures is rare B-decays as, in our opinion, experiments in e^+e^- annihilation and $p\bar{p}$ collisions are at the threshold of discovery in this sector. Rare B-decays involve flavour changing neutral current (FCNC) processes and in SM they are governed by one-loop graphs (penguins and boxes). They provide information on the properties of the top quark, in particular its mass and the three CKM matrix-elements $(V_{ti}; i = d, s, b)$. It should be recalled here that the $|\Delta B| = 2$ FCNC processes in B-physics, inducing the mass mixing in the neutral meson sector B_d^0-$\overline{B_d^0}$ and B_s^0-$\overline{B_s^0}$, have already been measured. Judging from the measured value of the phenomenologically relevant parameter in the B_d^0-$\overline{B_d^0}$ sector, $x_d = (\Delta M/\Gamma)_d = 0.67 \pm 0.10$ [15], and increasing experimental evidence that the mixing in the B_s^0-$\overline{B_s^0}$ sector is substantial, perhaps maximal, these processes are anything but rare! We shall not discuss the mass-mixings here in detail, but do take into account the constraints provided by them on the CKM matrix-elements. Our emphasis is on the so-called penguin (graph) dominated B-physics, inducing the $|\Delta B| = 1, \Delta Q = 0$ transitions. Examples of such transitions are radiative rare B-decays, which at the quark level can be represented as $b \to (s, d) + \gamma$, and the ones involving dileptons, such as $b \to (s, d) + \ell^+\ell^-$ $(\ell = e, \mu)$ and $b \to (s, d) + \nu\bar{\nu}$. Like their charged current (CC) counterparts, the inclusive rates and final state distributions in the FCNC rare B-decays can be calculated in perturbative QCD, which is the theoretical framework relied upon heavily in these lectures. Further, one could use phenomenological models already employed successfully in the analysis of CC data to incorporate B-meson wave function effects and get a fairly dependable profile of the inclusive

final states in rare B-decays. A good part of these lectures is devoted to elaborate the applications of perturbative QCD along these lines.

Exclusive rare B-decays are also discussed in these lectures. We review essentially two methods. First, using vector meson dominance of the inclusive hadron spectrum in the decays $B \to X_s + \gamma$ in the threshold region $(m_K + m_\pi) \leq m(X_s) \leq 1.0$ GeV gives an estimate of the decay rate for $B \to K^* + \gamma$. Likewise, assuming that the decays $B \to X_d + \gamma$ in the mass range $2m_\pi \leq m(X_d) \leq 1.0$ GeV are dominated by the exclusive channel $B \to \rho + \gamma$, gives the branching ratio for this channel. The assumption of vector meson dominance in this mass range is reasonable, since there is plenty of experimental evidence for such dominance from low energy experiments [13] and D-meson semileptonic decays [16,17,18]. However, probably these are the only radiative decay modes of the B-meson whose branching ratios can be estimated from the inclusive rates and spectra in this way. For higher invariant mass regions of X_d and X_s, there are just too many channels contributing to be able to extract a reliable number in any given decay channel.

Second, we discuss exclusive rare B-decays calculated using the heavy quark effective theory HQET [19,20,21]. For an excellent review of the HQET methods and applications we refer to the review by Mannel [23]. The usefulness of the HQET methods in rare B-decays is at present rather limited. Since they involve the so-called heavy to light transitions, reliable relations can be obtained only in the static b-quark limit. For example, one can relate rare B-decays, like $B \to K^* + \gamma$, and the CKM-suppressed CC decays such as $B \to \rho + \ell\nu_\ell$ [22,24]. There are, however, hardly any data available at present to make quantitative predictions. One could treat, for illustrative purposes, both the b and s quarks as heavy. This then allows to describe a large number of exclusive rare B-decays and the semileptonic decays of B and D mesons in terms of a single Isgur-Wise form factor [20]. It is, however, to be expected that there will be significant power corrections of $O(\Lambda/m_s)$ in such relations. Since these corrections have yet to be calculated, the results presented below are at best semi-quantitative. A test case for the importance of such power corrections is the semileptonic decay $D \to K^*\ell\nu_\ell$. The last word on the predictions of HQET for this decay is not yet out, since the experimental situation finds iteself very much in a state of flux [16,18]. The present parametrizations of the Isgur-Wise function are based on data from D-decays, which necessarily involve large extrapolation in the momentum space, in particular for estimating the decay $B \to K^* + \gamma$. The phenomeological predictions for rare B-decays can be firmed considerably when data on the CKM-suppressed CC B-decays become available.

These lectures are organized as follows: In section 2, we discuss the inclusive radiative rare B-decays, $B \to X_s + \gamma$ and $B \to X_d + \gamma$. The principal focus in this section is on estimating the inclusive energy-momentum profile of the final staes in rare B-decays. This is done by computing the leading QCD contribution to the inclusive photon energy spectrum, which is then supplemented by a wave-function model constrained by data in the CC semileptonic decay. In section 3, we discuss the FCNC semileptonic decays $b \to (s, d) + \ell^+\ell^-$ $(\ell = e, \mu)$ and $b \to (s, d) + \nu\bar{\nu}$. Since in this case, one has non-trivial decay distributions already at the lowest order, we don't discuss the effects of the higher order QCD bremsstrahlung processes. Application of QCD in this case is restricted to the evaluation of the improved Wilson coefficients. In section 4, we describe some applications of HQET in selected exclusive rare B-decays. Experimental limits are also listed in this section. A brief outlook is given in section 5.

2 RADIATIVE RARE B-DECAYS

We start by discussing the dominant FCNC inclusive B-decays. Such processes (as far as the short-distance contribution is concerned) are forbidden at the tree level in the SM Lagrangian but are allowed at the one-loop order. They have received quite a bit of theoretical interest in the last decade [25]-[44], since they serve both as precision tests of the Standard Model and windows on possible new physics. Here, we shall concentrate on the SM physics only and refer to a recent review covering the non-SM aspects of B-decays [45]. We enumerate the processes of interest in B-decays, define the effective Hamiltonians that govern them, and review the one-loop renormalization group (RG) improvement of the relevant Wilson coefficients of the operators in these Hamiltonians. This framework is then employed to calculate the inclusive rates and the energy-momentum profile of the decay products, using perturbative QCD and a B-meson wave function model.

In terms of the quark transitions, the main FCNC B-decays are the following:

1. $b \to (s,d) + \gamma$
2. $b \to (s,d) + \gamma + g$
3. $b \to (s,d) + g$
4. $b \to (s,d) + \ell^+\ell^- \ (\ell = e,\mu)$
5. $b \to (s,d) + \nu\bar{\nu}$

Of these, the most difficult to measure experimentally are the ones involving the hadronic final states $b \to (s,d) + g$, since they don't have a clean signature to be detected from the dominating CC decays $b \to u\bar{u}d$. So, we shall mostly neglect them and concentrate on the rest in the above list. The QCD improvements are usually done in the framework of an effective theory obtained by integrating out the heavy degrees of freedom, namely the top quark and the $W^\pm$ bosons. To be precise, these corrections are calculated in the leading logarithm approximation (LLA) since only in this approximation does the effective theory (with 5 quarks) match with the full theory (with 6 quarks and the $W^\pm$-bosons). As it will become clear from the discussion below, this matching is done in terms of the Wilson coefficients of the operators entering the effective Hamiltonian. This improved effective Hamiltonian incorporating the leading order RG-improvement is the basis of all phenomenological studies presented here. We remark that the gluon bremsstrahlung corrections, such as $b \to (s,d)+\gamma+g$, are required to get non-trivial photon energy spectra. Incorporating the QCD bremsstrahlung corrections and the virtual correction to $b \to (s,d) + \gamma$, using the one-loop improved effective Hamiltonian, amounts to incorporating the next-to leading order QCD corrections in the decays $B \to X_s + \gamma$ and $B \to X_d + \gamma$. The next-to-leading order corrections modify the rates for the inclusive decays $B \to X_d + \gamma$ and $B \to X_s + \gamma$, and their quantitative estimates are discussed below.

2.1 The Decays $b \to (s,d) + \gamma$: Lowest Order Contributions

We start with the lowest order (1-loop) calculations for the FCNC radiative decays $b \to (s,d) + \gamma$. Due to their similarity with the transitions $b \to s + X$ we shall discuss the

$b \to d + X$ transitions only when there are non-trivial differences. The matrix element for the process $b \to s + \gamma$ in the lowest order can be written as:

$$\mathcal{M}(b \to s\ +\gamma) = \frac{G_F}{\sqrt{2}}\frac{e}{2\pi^2}\sum_i V_{ib}V_{is}^* F_2^i(x_i)\, q^\mu \epsilon^\nu \bar{s}\sigma_{\mu\nu}(m_b R\ +\ m_s L)b \tag{1}$$

where G_F is the Fermi coupling constant, $L = (1-\gamma_5)/2$, $R = (1+\gamma_5)/2$, $x_i = m_i^2/m_W^2$, q_μ and ϵ_μ are, respectively, the photon four-momentum and polarization vector, and the sum is over the quarks, u, c, and t. The CKM matrix elements V_{ij} appearing above are defined in the Wolfenstein parametrization [46]:

$$V_{\rm CKM-W} = \begin{pmatrix} 1-\frac{1}{2}\lambda^2 & \lambda & A\lambda^3(\rho - i\eta) \\ -\lambda & 1-\frac{1}{2}\lambda^2 & A\lambda^2 \\ A\lambda^3(1-\rho-i\eta) & -A\lambda^2 & 1 \end{pmatrix} \tag{2}$$

The representation, $V_{\rm CKM-W}$, has three real parameters A, λ, and ρ, and a phase η, whose current values will be discussed below. The Inami-Lim function $F_2(x_i)$ derived from the penguin diagrams is given by [47]:

$$F_2(x) = \frac{x}{24(x-1)^4}\left[6x(3x-2)\log x - (x-1)(8x^2+5x-7)\right] \tag{3}$$

where we have dropped the superscript on F_2, and in writing the expression for $F_2(x_i)$ above we have left out terms of order $O(m_s/mb)$. For small x_i one has $F_2(x_i) \sim x_i$, hence the contribution of the u and c quarks in Eq. (1) can be neglected. Retaining only the top quark contribution in the amplitude, we have:

$$\mathcal{M}(b \to s\ +\gamma) = \frac{G_F}{\sqrt{2}}\frac{e}{2\pi^2}\lambda_t\, F_2(x_t)\, q^\mu \epsilon^\nu \bar{s}\sigma_{\mu\nu}(m_b R\ +\ m_s L)b \tag{4}$$

with $\lambda_t \equiv V_{tb}V_{ts}^*$. The amplitude for the CKM-suppressed FCNC radiative transition $b \to d + \gamma$ is obtained by replacing the s-quark variables by the d-quark ones. The CKM factor in this case is $\xi_t \equiv V_{tb}V_{td}^*$. The widths $\Gamma(\ b \to s + \gamma)$ and $\Gamma(\ b \to d + \gamma)$ in the lowest order are:

$$\Gamma(b \to s + \gamma) = |\lambda_t|^2 \frac{G_F^2 m_b^5 \alpha}{32\pi^4}|F_2(x_t)|^2 \tag{5}$$

$$\Gamma(b \to d + \gamma) = |\xi_t|^2 \frac{G_F^2 m_b^5 \alpha}{32\pi^4}|F_2(x_t)|^2 \tag{6}$$

where we have dropped terms of $O(m_s/m_b)$ and $O(m_d/m_b)$ in the phase space also. From the expression for $F_2(x_t)$ it is easy to see that for low values of x_t ($x_t \Lambda 1$) one has a quartic suppression in m_t of the decay rates $\Gamma(\ b \to s + \gamma)$ and $\Gamma\ (\ b \to d + \gamma)$; this goes over to a constant behaviour for $x_t \gg 1$. So, while intrinsically there is a large m_t-dependence in the decay widths for both the $b \to s + \gamma$ and $b \to d + \gamma$ transitions, this dependence in the m_t-range of present phenomenological interest, 100 GeV $< m_t <$ 200 GeV, is rather modest, as can be seen in Fig. 1.

The rates for rare B-decays may be expressed in terms of the branching ratio for the inclusive CC semileptonic B-decays $B \to (X_c,\ X_u)\ell\nu_\ell$, which have been well measured

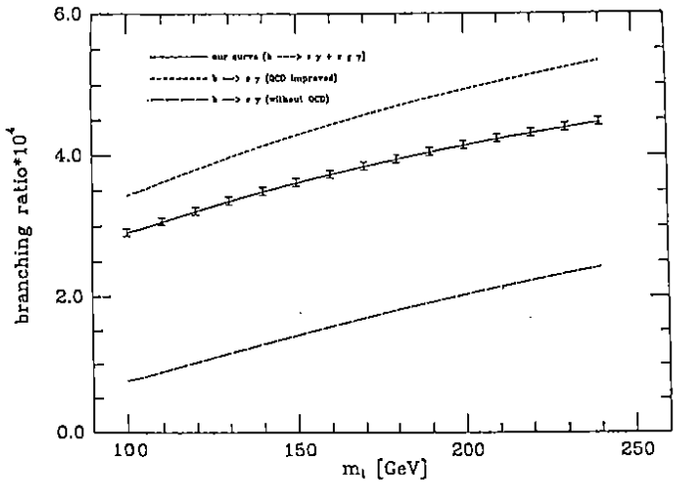

Figure 1: Inclusive branching ratio for the decays $B \to X_s + \gamma$ as a function of the top quark mass m_t. The charm quark mass dependence for $m_c = 1.5 \pm 0.2\ GeV$ is indicated by error bars. Also shown are the lowest order (i.e. without QCD corrections) and the leading order QCD-improved results for the two-body decays $b \to s + \gamma$ (from [38]).

(here and henceforth we use the quark flavour in the transition $b \to q$ to specify the resulting hadronic state, X_q). This removes the annoying m_b^5 dependence in their rates. In the approximation of keeping the dominant $b \to c\ell\nu_\ell$ contribution, one has:

$$BR(b \to s + \gamma) = 6\frac{\alpha}{\pi}\frac{|\lambda_t|^2}{|V_{bc}|^2}\frac{|F_2(x_t)|^2}{f(m_c/m_b)}(0.12) \tag{7}$$

$$\frac{BR(b \to d + \gamma)}{BR(b \to s + \gamma)} = \frac{|V_{td}|^2}{|V_{ts}|^2} \tag{8}$$

where the function $f(m_c/m_b)$ is the the phase space factor in the CC semileptonic decay $b \to c + \ell\nu_\ell$. Numerically, $f(m_c/m_b) \simeq 0.44$. The number in the paranthesis in Eq. (7) corresponds to the average B-hadron semileptonic branching ratio given in the PDG tables [13]. The branching ratio for $b \to s + \gamma$ as a function of m_t is shown in Fig. 1, and we note that it does not depend on the CKM-matrix elements since $|V_{ts}|^2/|V_{bc}|^2 = 1$. To quote a number from this figure, one gets BR($b \to s + \gamma$) $\simeq 1.5 \times 10^{-4}$ for $m_t = 150\ GeV$, for the lowest order (i.e. no QCD corrections). We shall estimate the ratio in Eq. (8) later, making use of the available constraints on the CKM matrix elements. As an order of magnitude, we expect this ratio to be $O(\lambda^2) \simeq 0.05$. We discuss first the leading order perturbative QCD corrections in the two-body decays $b \to (s,d) + \gamma$ (i.e. QCD renormalization of the Wilson coefficients) and then take up the next-to-leading order corrections due to the gluon bremsstrahlung contributions from the decays $b \to (s,d) + \gamma + g$, as well as, the virtual corrections to $b \to (s,d) + \gamma$. This will lead us to the discussion of the inclusive photon energy spectra.

2.2 QCD Corrections to the Decay $b \to s + \gamma$

To implement QCD corrections, an appropriate operator basis has to be defined first. One keeps only the operators with the lowest (mass) dimensions since the higher dimension operators are power suppressed by terms of $O(m_b/m_t)$ and $O(m_b/m_W)$. The list of dimension-6 operators consists of four fermion operators, involving the light quark fields and the covariant derivatives of the SM $[SU(3)_c \times SU(2)_L \times U(1)_Y]$ groups. It also includes the magnetic moment operators involving the photon and gluon fields. Without any further constraints one has quite a large number of operators that contribute to H_{eff} and calculating the anomalous dimension matrix is highly non-trivial. However, since the initial and final particles (quarks, photons and gluons) in the decays of interest are always teken to be on the mass-shell, one could use the equations of motion to get rid of the covariant derivatives and reduce the number of independent operators. To leading order in the small (weak)-mixing angles, a complete set of dimension-6 operators relevant for the processes $b \to s + \gamma$ and $b \to s + \gamma + g$ is contained in the effective Hamiltonian

$$H_{eff}(b \to s + \gamma) = -\frac{4G_F}{\sqrt{2}}\lambda_t \sum_{j=1}^{8} C_j(\mu)\,\hat{O}_j(\mu) \tag{9}$$

with $C_j(\mu)$ being the Wilson coefficients evaluated at the scale μ. The various operators are defined as:

$$\begin{aligned}
\hat{O}_1 &= (\bar{c}_{L\beta}\gamma^\mu b_{L\alpha})(\bar{s}_{L\alpha}\gamma_\mu c_{L\beta}) \\
\hat{O}_2 &= (\bar{c}_{L\alpha}\gamma^\mu b_{L\alpha})(\bar{s}_{L\beta}\gamma_\mu c_{L\beta}) \\
\hat{O}_3 &= (\bar{s}_{L\alpha}\gamma^\mu b_{L\alpha})\left[(\bar{u}_{L\beta}\gamma_\mu u_{L\beta}) + \cdots + (\bar{b}_{L\beta}\gamma_\mu b_{L\beta})\right] \\
\hat{O}_4 &= (\bar{s}_{L\alpha}\gamma^\mu b_{L\beta})\left[(\bar{u}_{L\beta}\gamma_\mu u_{L\alpha}) + \cdots + (\bar{b}_{L\beta}\gamma_\mu b_{L\alpha})\right] \\
\hat{O}_5 &= (\bar{s}_{L\alpha}\gamma^\mu b_{L\alpha})\left[(\bar{u}_{R\beta}\gamma_\mu u_{R\beta}) + \cdots + (\bar{b}_{R\beta}\gamma_\mu b_{R\beta})\right] \\
\hat{O}_6 &= (\bar{s}_{L\alpha}\gamma^\mu b_{L\beta})\left[(\bar{u}_{R\beta}\gamma_\mu u_{R\alpha}) + \cdots + (\bar{b}_{R\beta}\gamma_\mu b_{R\alpha})\right] \\
\hat{O}_7 &= (e/16\pi^2)\,\bar{s}_\alpha\,\sigma^{\mu\nu}\,(m_b R + m_s L)\,b_\alpha\,F_{\mu\nu} \\
\hat{O}_8 &= (g_S/16\pi^2)\,\bar{s}_\alpha\,\sigma^{\mu\nu}\,(m_b R + m_s L)\,T^A_{\alpha\beta}\,b_\beta\,G^A_{\mu\nu}
\end{aligned} \tag{10}$$

e and g_S denote the QED and QCD coupling constant, respectively. Pertubative QCD corrections, contained in the Wilson coefficients $C_j(\mu)$, have been evaluated to leading logarithmic accuracy. It is known that the Wilson coefficients of the operators $\hat{O}_3, ..., \hat{O}_6$ get contributions from operator mixing only; as these coefficients are numerically small [33,36,37] their effect is usually neglected. The coefficients $C_1(\mu), C_2(\mu), C_7(\mu)$ and $C_8(\mu)$, obtained by integrating out the top quark and the W-boson simultaneously, are given in refs. [33,35]. At $\mu = m_b$, which is the relevant scale for the b quark decay, these coefficients read as follows:

$$\begin{aligned}
C_1(m_b) &= \frac{1}{2}\left[\eta^{-6/23} - \eta^{12/23}\right] C_2(m_W) \\
C_2(m_b) &= \frac{1}{2}\left[\eta^{-6/23} + \eta^{12/23}\right] C_2(m_W) \\
C_7(m_b) &= \eta^{-16/23}\left\{C_7(m_W) - \frac{58}{135}\left[\eta^{10/23} - 1\right] C_2(m_W) - \frac{29}{189}\left[\eta^{28/23} - 1\right] C_2(m_W)\right\} \\
C_8(m_b) &= \eta^{-14/23}\left\{C_8(m_W) - \frac{11}{144}\left[\eta^{8/23} - 1\right] C_2(m_W) + \frac{35}{234}\left[\eta^{28/23} - 1\right] C_2(m_W)\right\}
\end{aligned} \tag{11}$$

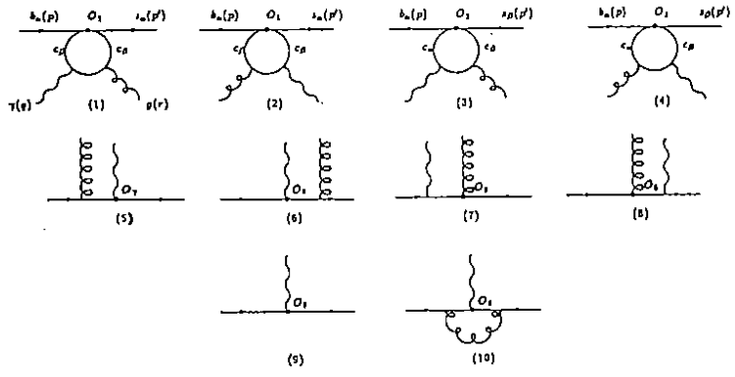

Figure 2: The Feynman diagrams contributing to the decays $b \to s+\gamma$ and $b \to s+\gamma+g$ (from [39]).

with $\eta = \frac{\alpha_S(m_b)}{\alpha_S(m_W)}$ being the ratio of the QCD coupling constants. At the scale $\mu = m_W$, where the matching conditions from the lowest order (1 loop) results are imposed [47], we have (again to leading logarithmic accuracy):

$$\begin{aligned} C_j(m_W) &= 0 \quad , \quad j = 1,3,4,5,6 \\ C_2(m_W) &= 1 \\ C_7(m_W) &= F_2(x) \\ C_8(m_W) &= -\frac{x}{8(x-1)^4}\left[6x\log x + (x-1)(x^2-5x-2)\right] \end{aligned} \tag{12}$$

with $x = m_t^2/m_W^2$. For the two-body decays $b \to s+\gamma$, only the magnetic moment operator $\hat{O}_7$ contributes and hence the QCD corrected rate can be represented by formulæ similar to the ones given above for the lowest order, with the function $F_2(x)$ replaced by the QCD corrected function $C_7(m_b)$. Taking into account only the two-body decays $b \to s+\gamma$, QCD-improvements boil down to a scaling of the Wilson coefficient of the magnetic moment operator, $C_7(m_W) \to C_7(m_b)$. The branching ratio for the decay $b \to s+\gamma$ (leading order QCD-improved) as a function of m_t is also shown in Fig. 1, as the topmost curve. The net result of these QCD corrections for the two-body radiative decay width is very significant, increasing the rate by ~ 6 for $m_t = 100\ GeV$ to ~ 3 for $m_t = 200\ GeV$, assuming $\Lambda_{QCD} = 200\ MeV$.

2.3 QCD Corrections to the Decay $b \to d+\gamma$

For the decays $b \to s+\gamma$ the effective Hamiltonian was written in the approximation $\lambda_u = 0$, which is reasonable since one can easily see that $\lambda_u \Lambda \lambda_c$, λ_t (where the CKM factors are defined as $\lambda_i \equiv V_{ib}V_{is}^*$). For the decays $b \to d+\gamma$ and $b \to d+\gamma+g$ the CKM factors λ_i are replaced by $\xi_i \equiv V_{ib}V_{id}^*$. Now ξ_u, ξ_c and ξ_t are all of the same order of magnitude, $O(\lambda^3)$,

and therefore the corresponding approximation $\xi_u = 0$ cannot be made any longer. It has been shown in [44] that the differences due to the inclusion of the ξ_u terms needed for the $b \to s+\gamma$ and $b \to s+\gamma+g$ decays can be most easily built in the framework discussed for the decay $b \to s+\gamma$ by modifying the operators $\hat{O}_1$ and $\hat{O}_2$, given earlier. The dimension-6 operator basis in this case is:

$$H_{eff}(b \to d+\gamma) = -\frac{4G_F}{\sqrt{2}}\xi_t \sum_{j=1}^{8} C_j(\mu)\, O_j(\mu) \quad , \tag{13}$$

The two modified operators O_1 and O_2 are now defined as [44]:

$$\begin{aligned} O_1 &= -\frac{\xi_c}{\xi_t}(\bar{c}_{L\beta}\gamma^\mu b_{L\alpha})(\bar{d}_{L\alpha}\gamma_\mu c_{L\beta}) - \frac{\xi_u}{\xi_t}(\bar{u}_{L\beta}\gamma^\mu b_{L\alpha})(\bar{d}_{L\alpha}\gamma_\mu u_{L\beta}) \\ O_2 &= -\frac{\xi_c}{\xi_t}(\bar{c}_{L\alpha}\gamma^\mu b_{L\alpha})(\bar{d}_{L\beta}\gamma_\mu c_{L\beta}) - \frac{\xi_u}{\xi_t}(\bar{u}_{L\alpha}\gamma^\mu b_{L\alpha})(\bar{d}_{L\beta}\gamma_\mu u_{L\beta}) \end{aligned} \tag{14}$$

The other operators $O_3, ..., O_8$ are identical to their counterparts $\hat{O}_3, ..., \hat{O}_8$ encountered in the decays $b \to s+\gamma+g$, with the obvious replacement of the fields $s \to d$. With the operators defined in this basis, the matching conditions $C_i(m_W)$ and the corresponding Wilson coefficients at the scale $\mu = m_b$, $C_i(m_b)$, are precisely the same for the decays $b \to d+\gamma$ as given above for the $b \to s+\gamma$ case [44]. The consequence of this is that the leading order QCD-improvement for the two-body decay amplitude $\mathcal{M}(b \to d+\gamma)$ is identical to the one for the decay $b \to s+\gamma$, since both involve just the rescaling of the Wilson coefficient $C_7(m_W) \to C_7(m_b)$. Thus, the QCD enhancement we discussed for the $b \to s+\gamma$ case previously, which amounts to a factor (3-6) in the m_t-range of interest, also applies for the $b \to d+\gamma$ decay. It follows that the ratio $\Gamma(b \to d+\gamma)/\Gamma(b \to s+\gamma)$ given above in the lowest order remains unrenormalized due to the leading-order QCD-corrections to the two-body processes. As we shall see in the next section, including QCD bremsstrahlung processes $b \to s+\gamma+g$ and $b \to d+\gamma+g$ will lead to non-factorizing corrections (in the CKM parameters) to the ratio of the inclusive decay rates $\Gamma(B \to X_d+\gamma)/\Gamma(B \to X_s+\gamma)$.

It should be remarked here that there are two approximations that have gone into the derivation of the QCD corrections to the Wilson coefficients sketched above. The first one is due to setting $m_W \approx m_t$ in the evaluation of $C_i(\mu)$, which amounts to neglecting the running of the QCD coupling $\alpha_S(Q^2)$ between m_t and m_W. Since the running is anyway small in the top quark mass range of current interest $89\ GeV < m_t < 200\ GeV$, the residual correction from this approximation is expected to be small (within 10%). These expectations have been confirmed in a recent calculation [48], in which an effective 5-quark Hamiltonian for the process $b \to s+\gamma$ has been obtained by integrating out first a heavy top quark with $m_t^2 \gg m_W^2$ and then integrating out the W-boson. The two-step integration procedure results in increasing the radiative decay width $\Gamma(b \to s+\gamma)$, (likewise for $\Gamma(b \to d+\gamma)$) by as much as 14% for $m_t = 250\ GeV$ and $\Lambda_{\overline{MS}} = 300\ MeV$. However, in view of the LLA nature of these calculations, their legitimacy is limited to such values of m_t which satisfy $log(m_t/m_W) \gg 1$. The second approximation is due to neglecting the effect of the mixing of the operators $\hat{O}_3 ... \hat{O}_8$ with the rest, which modifies the expression given above for $C_7(m_b)$. This approximation (truncating the operator basis) has also been recently investigated and the resulting correction to the decay rate $\Gamma(b \to s+\gamma)$ is found to be $O(10\%)$ [37], reducing

the branching ratios presented above. Same remarks apply for the decay rate $\Gamma(b \to d+\gamma)$. Since the two mentioned corrections are both $O(10\%)$, and they have opposite signs, the radiative rare b-decay branching ratios presented in Fig. 1 are not significantly altered.

2.4 QCD Bremsstrahlung Processes $b \to s+\gamma+g$ and $b \to d+\gamma+g$

We first sketch here the main points of the perturbative QCD calculations for the process $b \to s+\gamma+g$ done in refs. [38,39], where dimensional regularization and (Landau gauge) were used. Analogous calculations done for $b \to d+\gamma+g$ in ref. [44] will be discussed in the later part of this section.

In the approximation of keeping only the contributions of the operators $\hat{O}_1, \hat{O}_2, \hat{O}_7$, and $\hat{O}_8$, the amplitude for the processes $b \to s+\gamma+g$ can be calculated from the diagrams shown in Fig. 2. The diagrams associated with $\hat{O}_1$ vanish due to the colour structure. Also, the coefficient of the operator $\hat{O}_8$ gets suppressed after including QCD effects and its contribution is neglected. It is quite adequate to keep the contributions associated with $\hat{O}_2$ and $\hat{O}_7$ only. Note, that the diagrams where only one boson (gluon or photon) is radiated from an internal quark line vanish in dimensional regularization and hence are not shown.

Concerning the photon energy spectra in the decays $b \to (s,d)+\gamma+g$, it is to be noted that they have a nonintegrable infrared singularity for the gluon energy $E_g \to 0$, or equivalently as $E_\gamma \to E_\gamma^{max}$. Adding the contributions of the virtual QCD corrections to the processes $b \to (s,d)+\gamma$ with their respective bremsstrahlung part, the singularity cancels [38]. The end-point spectra, however, show sensitivity to the left over effects of the (cancelled) infrared singularity, with the photon-energy distribution $\frac{d\Gamma}{dx_\gamma}$ rising very steeply near the end-point, $x_\gamma \simeq 1$ (here x_γ is the fractional energy of the photon, $x_\gamma = E_\gamma/E_\gamma^{max}$). To remedy this, one often resorts to (an all order) resummation of the leading (infrared) logarithms. The resummed theory provides a more reliable description of the spectra near the end-point. We reproduce below the essential steps in the derivation of the photon energy spectrum and discuss the exponentiation procedures used to estimate the end-point spectrum in the decays $b \to s+\gamma(+g)$, given in ref. [38,39,44]. The corresponding derivation for the decays $b \to d+\gamma(+g)$, recently obtained in [44], are discussed subsequently.

Following ref. [38,39], one can express the photon energy spectrum as a sum of the following parts:

$$\frac{d\Gamma}{dx_\gamma} = \frac{d\Gamma_F}{dx_\gamma} + \frac{d\Gamma_7}{dx_\gamma} \tag{15}$$

The first term on the r.h.s of Eq. (15) contains the square of the matrix element of the operator $\hat{O}_2$ and the interference term of $\hat{O}_2$ and $\hat{O}_7$ and can be written as a one-dimensional integral over the gluon energy in the process $b \to s+\gamma+g$ [38]:

$$\begin{aligned}
\frac{d\Gamma_F}{dx_\gamma} &= \frac{G_F^2\,|\lambda_t|^2\,\alpha\,\alpha_S\,(1-r)}{1536\,\pi^5} \int_{E_g^-}^{E_g^+} (\hat{\tau}_{22}+\hat{\tau}_{27})\,dE_g \\
\hat{\tau}_{22} &= \frac{8}{9}\,C_2^2(\mu)\,(qq')^2\,|\kappa|^2\,\left\{(m_b^2-m_s^2)^2 - 2(m_s^2+m_b^2)\,(qq')\right\} \\
\hat{\tau}_{27} &= \frac{64}{3}\,C_2(\mu)\,C_7(\mu)\,(qq')^2\,\mathrm{Re}(\kappa)\,\left\{\frac{m_s^2\,m_b^2\,(qq')}{(pq')\,(p'q')} - (m_s^2+m_b^2)\right\} \quad .
\end{aligned} \tag{16}$$

The limits of the E_g integration are:

$$E_g^- = \frac{m_b}{2}(1-r)(1-x_\gamma) \quad ; E_g^+ = \frac{m_b}{2}\,\frac{(1-r)(1-x_\gamma)}{1-\xi} \quad ; \quad r = (m_s/m_b)^2 \quad ; \xi = x_\gamma(1-r) \quad ; \tag{17}$$

and q, q', p and p' denote the four-momenta of the photon, gluon, b-quark and s-quark, respectively. The function κ is defined as:

$$\kappa = \frac{4\,(2\,G(t)+t)}{(qq')\,t} \quad ,$$

where $t = \frac{2(qq')}{m_b^2}$ and $G(t)$ is defined by the integral

$$G(t) = \int_0^1 \frac{dy}{y}\,\log(1-t\,y\,(1-y)-i\epsilon) \tag{18}$$

which yields:

$$\begin{aligned}
G(t) &= -2\,\mathrm{atan}^2\left(\sqrt{\frac{t}{4-t}}\right); \quad t<4 \\
G(t) &= -\pi^2/2 + 2\log^2\left(\frac{\sqrt{t}+\sqrt{t-4}}{2}\right) - 2i\pi\log\left(\frac{\sqrt{t}+\sqrt{t-4}}{2}\right); \quad t>4
\end{aligned} \tag{19}$$

The second term on the r.h.s of Eq. (15) involves the matrix element squared of the operator $\hat{O}_7$. For the sake of clarity and also to remain close to the procedure adopted in ref. [39], we split the second term into two parts:

$$\frac{d\Gamma_7}{dx_\gamma} = \frac{d\Gamma_A}{dx_\gamma} + \frac{d\Gamma_B}{dx_\gamma} \tag{20}$$

The term $\frac{d\Gamma_A}{dx_\gamma}$ is the finite part of the bremsstrahlung spectrum and it can be expressed as:

$$\begin{aligned}
\frac{d\Gamma_A}{dx_\gamma} &= C_0\,\frac{\alpha_S}{3\pi}\,\left\{\frac{x_\gamma(2x_\gamma^2-5x_\gamma-1)(1-r)}{1-\xi} - 2(1+x_\gamma)\log(1-\xi)\right. \\
&\qquad \left. + \frac{(1-r)\,x_\gamma\,(1-x_\gamma)\,(2x_\gamma-1)}{(1-\xi)^2}\right\}
\end{aligned} \tag{21}$$

$$C_0 = (1-r)^3\,(1+r)\,\frac{m_b^6}{32\pi^4}\,\alpha\,G_F^2\,|\lambda_t|^2\,C_7^2(\mu) \tag{22}$$

It is clear from Eq. (21) that this term is not going to yield the leading ($\propto \frac{1}{(1-x_\gamma)}$) contribution. One has to look at the anatomy of the term $\frac{d\Gamma_B}{dx_\gamma}$, which receives the remaining contributions from the bremsstrahlung diagrams. In addition, there is also a term proportional to $\delta(1-x_\gamma)$ in $\frac{d\Gamma_B}{dx_\gamma}$ stemming from the process $b \to s+\gamma$ including virtual corrections. Both these contributions are individually infrared singular but finite in the sum in a distribution sense. The expression for $x_\gamma \neq 1$, after removing the infrared regularization, can be shown to be the following [39]:

$$\frac{d\Gamma_B}{dx_\gamma} = C_0\,\frac{\alpha_S}{3\pi}\,\frac{x_\gamma}{1-x_\gamma}\,\left\{-4 - \frac{4r}{1-\xi} - \frac{4}{\xi}(1+r)\log(1-\xi)\right\} \tag{23}$$

This is the leading contribution to the photon energy spectrum, in the region $x_\gamma \to 1$ for $m_s \neq 0$ (i.e. $r \neq 0$). In terms of the parameter s_0, the integral of the term $\frac{d\Gamma_B}{dx_\gamma}$ is:

$$\Gamma_B(s_0) \equiv \int_{s_0}^{1} dx_\gamma \frac{d\Gamma_B}{dx_\gamma} \tag{24}$$

The result of this integration can be obtained analytically:

$$\begin{aligned}
\Gamma_B(s_0) &= C_0 \left\{1 - \frac{4\alpha_S}{3\pi} A(s_0) + \frac{\alpha_S}{3\pi} B(s_0)\right\} \Theta(1-s_0) \qquad (25)\\
A(s_0) &= 2\log(1-s_0) + \frac{1+r}{1-r}\log\eta_0 \log(1-s_0)\\
B(s_0) &= 5\log(r) - 8\log(1-r) - 4s_0 + \frac{4}{1-r}\log\eta_0 + \\
&\quad + \frac{1+r}{1-r}\Big[-8\log r + 4\log r\log(1-r) - \frac{4\pi^2}{3} + 4\mathrm{Li}(r/\eta_0) + \\
&\qquad 4\mathrm{Li}(r) + 2\log^2\eta_0 - 4\log\eta_0\log(1-r)\Big] \qquad (26)
\end{aligned}$$

where,

$$\eta_0 = 1 - s_0(1-r) \quad , \quad \mathrm{Li}(x) = -\int_0^x \frac{dt}{t}\log(1-t) \quad . \tag{27}$$

One could exponentiate the leading log terms which are defined by the function $A(s_0)$. Since, $\frac{d\Gamma_B}{dx_\gamma} = -\frac{d\Gamma_B}{ds_0}|_{s_0=x_\gamma}$, an exponentiated version follows:

$$\begin{aligned}
\frac{d\Gamma_B^{exp}}{dx_\gamma} &= \frac{4\alpha_S}{3\pi} C_0 \exp\left\{-\frac{4\alpha_S}{3\pi}\log(1-x_\gamma)\left[2 + \frac{1+r}{1-r}\log(1-\xi)\right]\right\} \\
&\quad \times \left\{\frac{2-\xi}{1-\xi} + \frac{1+r}{1-\xi}\log(1-x_\gamma) - \left(1 + \frac{\alpha_S}{3\pi}B(x_\gamma)\right)\right. \\
&\quad \left. \times \left[\frac{2}{1-x_\gamma} + \frac{1+r}{1-r}\frac{\log(1-\xi)}{1-x_\gamma} + \frac{(1+r)\log(1-x_\gamma)}{1-\xi}\right]\right\}
\end{aligned} \tag{28}$$

with $B(x_\gamma) = B(s_0 \to x_\gamma)$. It can be easily checked that after integration this term leads to $\Gamma_B(s_0)$. Also, expanding the exponential and keeping terms of $O(\alpha_s)$ it reproduces the term given in Eq. (23) above. As exponentiation is required only near the end-point $x_\gamma \to 1$, the exponentiated form is used in the region $x_\gamma > x_{crit}$ only. For numerical calculations in refs. [39,44], a value $x_{crit} = 0.85$ was assumed. The inclusive spectrum for the entire x_γ-range is obtained by the following expression:

$$\frac{d\Gamma}{dx_\gamma} = \frac{d\Gamma_F}{dx_\gamma} + \frac{d\Gamma_A}{dx_\gamma} + \Theta(x_{crit}-1)\frac{d\Gamma_B}{dx_\gamma} + \Theta(1-x_{crit})\frac{d\Gamma_B^{exp}}{dx_\gamma} \tag{29}$$

where the required expressions are given in Eqs. (16), (21), (23), and (28). Below, we discuss a different exponentiation procedure which is more suitable for the case $r = 0$. The resulting photon spectra and the dependence on the exponentiation procedure will be discussed only after the specification of a non-perturbative model.

We take up the decay $b \to d+\gamma+g$ next. As stated in the previous section, one now works with the modified operators O_1 and O_2. It is to be noted that in the diagrams associated with O_1 and O_2 in Fig. 2 (with the obvious change $s \to d$) both the $u-$ and c-quark propagate in the loop. Also, like the decay $b \to s+\gamma+g$, it is adequate to take into account only the contributions of the diagrams associated with O_2 and O_7. One can again split the differential decay width into two pieces as done in Eq. (15). The expression for $\frac{d\Gamma_F}{dE_\gamma}$ for the decay $b \to d+\gamma+g$ can be written in the same form as the corresponding expression for the decay $b \to s+\gamma+g$ with the substitution $|\lambda_t|^2 \to |\xi_t|^2$ in Eq. (16), giving [44]:

$$\begin{aligned}
\frac{d\Gamma_F}{dx_\gamma} &= \frac{G_F^2 |\xi_t|^2 \alpha\, \alpha_S (1-r)}{1536\,\pi^5} \int_{E_g^-}^{E_g^+} (\tau_{22} + \tau_{27})\, dE_g \\
\tau_{22} &= \frac{8}{9} C_2^2(\mu)\,(qq')^2\,|\tilde\kappa|^2 \left\{(m_b^2 - m_d^2)^2 - 2(m_d^2 + m_b^2)(qq')\right\} \quad , \\
\tau_{27} &= \frac{64}{3} C_2(\mu)\, C_7(\mu)\,(qq')^2\,\mathrm{Re}(\tilde\kappa) \left\{\frac{m_d^2 m_b^2\,(qq')}{(pq')\,(p'q')} - (m_d^2 + m_b^2)\right\} \quad , \\
\tilde\kappa &= -\frac{\xi_c}{\xi_t}\kappa - \frac{\xi_u}{\xi_t}\frac{4}{qr}
\end{aligned} \tag{30}$$

and the various variables and functions have already been defined. We draw attention to the non-trivial dependence of the functions τ_{22} and τ_{27} on the CKM factors ξ_c and ξ_u. In the Wolfenstein parametrization one has:

$$\begin{aligned}
\frac{\xi_c}{\xi_t} &= \frac{(\rho-1)+i\eta}{(1-\rho)^2+\eta^2} \\
\frac{\xi_u}{\xi_t} &= \frac{(\rho-i\eta)(1-\rho-i\eta)}{(1-\rho)^2+\eta^2}
\end{aligned} \tag{31}$$

It is obvious from this explicit dependence that the photon energy spectrum in the decays $b \to d+\gamma+g$ is sensitive to both ρ and the CP-violating phase η. If one had kept only the contribution due to O_7, which is the case for the two-body decay $b \to d+\gamma$, one would not have noticed this dependence due to the neglect of the subleading terms. The possibilty of CP-violation in rare radiative B-decay rates was pointed out in ref. [49], where, however, the imaginary part of the bremsstrahlung diagrams from $b \to d+\gamma+g$ was not considered. A reliable estimate of the CP-violating asymmetry in both the rates and spectra has yet to be obtained. We shall not pursue the CP-violation aspect any further. Returning to the derivation of the photon energy spectrum in the decay $b \to d+\gamma+g$, we note that the $d\Gamma_7$ contribution is identical (up to the replacement $m_s \to m_d$) to the $b \to s+\gamma+g$ case. It has a part due to the exchange of a virtual gluon and a part due to gluon bremsstrahlung. These were separately discussed above for the decay $b \to s+\gamma+g$. We give here the expression for the sum in terms of the parameter s_0 [44]:

$$\Gamma_7(s_0) \equiv \int_{s_0}^{1} \frac{d\Gamma_7}{dx_\gamma} dx_\gamma \quad . \tag{32}$$

Doing the indicated x_γ-integration, one gets:

$$\Gamma_7(s_0) = V\left(1 + \frac{\alpha_s}{3\pi}\Omega\right)\Theta(1-s_0) \quad ,$$

$$V = (1-r)^3(1+r)\frac{m_b^5}{32\pi^4}\alpha G_F^2|\xi_t|^2 C_7^2 \quad . \tag{33}$$

To exponentiate the end-point spectrum, we now split Ω into two contributions: $\Omega = \Omega_1 + \Omega_2$, with the two given by:

$$\begin{aligned}\Omega_1 &= \frac{1+r}{1-r}\left[2\log^2\eta_0 - 4\log\eta_0\log(1-s_0)\right. \\ &\left. +\frac{4}{1-r}\log\eta_0 - 8\log(1-s_0) + \frac{11r-3}{(1-r)^3}\log\eta_0\right] \quad ,\end{aligned} \tag{34}$$

$$\begin{aligned}\Omega_2 &= -4s_0 - 8\log(1-r) + 4\frac{1+r}{1-r}\left(\log(1-r)\log\left(\frac{r}{\eta_0}\right) - \frac{\pi^2}{3} + \mathrm{Li}\left(\frac{r}{\eta_0}\right) + \mathrm{Li}(r)\right) \\ &+\frac{1}{(1-r)^3}\left[(3r^2-21r+6)(\eta_0-r) + (1+3r)(\eta_0^2-r^2) - \frac{2}{3}(\eta_0^3-r^3)\right. \\ &\quad -\frac{(1-r^2)(1-s_0)}{\eta_0} - 2(1-r)(2-r)\left(\eta_0\log\eta_0 - r\log r\right) \\ &\left. \quad +(1-r)(\eta_0^2\log\eta_0 - r^2\log r) - r(13r^2-23r+18)\log r\right] \quad .\end{aligned} \tag{35}$$

Here $\eta_0 \equiv 1-(1-r)s_0$. Note that Ω_2 is finite for $s_0 \to 1$ both for $r=0$ and $r \neq 0$. In Ω_1, for $r \neq 0$ only the terms proportional to $\log(1-s_0)$ are singular as $s_0 \to 1$. We recall here that in the decay $b \to s+\gamma+g$, we had tacitly assumed that $m_s \neq 0$, in which case the leading singularity was a single log. Accordingly, only the terms proportional to $\log(1-s_0)$ in Ω_1 were exponentiated, giving rise to the function $d\Gamma_B^{exp}$, discussed earlier. However, in the limit $r \to 0$ (which is more appropriate for the case $b \to d+\gamma$ and $b \to d+\gamma+g$), the variable η_0 becomes $1-s_0$ and therefore $\log\eta_0 \to \log(1-s_0)$, giving rise to a double log singularity in Ω_1. This is the essential difference in the limiting behaviour for the $r=0$ and $r \neq 0$ cases. In order to have a smooth transition from the $r \neq 0$ to the $r=0$ case, it has been suggested in ref. [44] that one could exponentiate the entire Ω_1 contribution (i.e. both the leading double log and the next-to-leading single log terms), giving:

$$\Gamma_7^{exp}(s_0) = V\left(1+\frac{\alpha_s}{3\pi}\Omega_2\right)\exp\left(\frac{\alpha_s}{3\pi}\Omega_1\right)\Theta(1-s_0) \quad . \tag{36}$$

The exponentiated version of the O_7 contribution to the photon energy spectrum then yields:

$$\frac{\Gamma_7^{exp}}{dx_\gamma}(x_\gamma) = -\frac{d\Gamma_7^{exp}(s_0)}{s_0}|_{s_0\to x_\gamma} \quad , \tag{37}$$

$$\frac{d\Gamma_7^{exp}}{dx_\gamma} = -V\frac{\alpha_s}{3\pi}\exp\left(\frac{\alpha_s}{3\pi}\Omega_1\right)\left\{\Omega_2' + \Omega_1'\left(1+\frac{\alpha_s}{3\pi}\Omega_2\right)\right\} \tag{38}$$

$$\begin{aligned}\Omega_1' &= -\frac{4}{\eta_0} + \frac{8}{1-s_0} + \frac{3-11r}{\eta_0(1-r)^2} \\ &+4\frac{1+r}{1-r}\left\{-\frac{(1-r)\log\eta_0}{\eta_0} + \frac{\log\eta_0}{1-s_0} + \frac{(1-r)\log(1-s_0)}{\eta_0}\right\}\end{aligned} \tag{39}$$

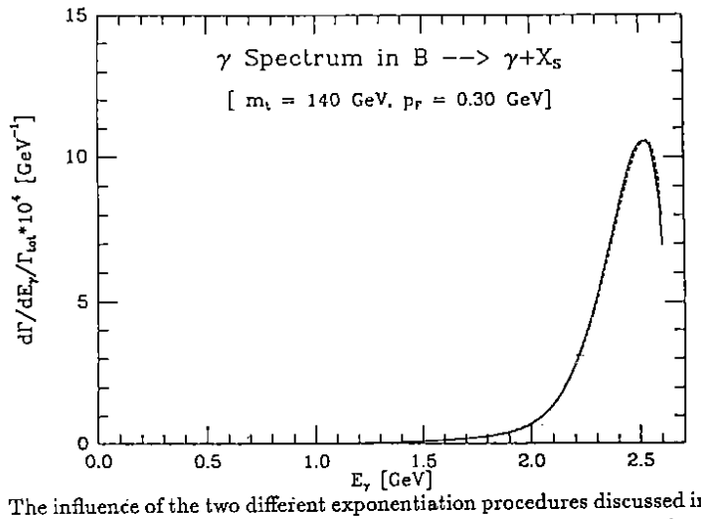

Figure 3: The influence of the two different exponentiation procedures discussed in the text on the photon energy spectrum is illustrated for the inclusive decay $B \to X_s\gamma$, after convolution with the B-meson wave-function (from [44]).

$$\begin{aligned}\Omega_2' &= -\frac{4(1+r)}{\eta_0}\log(1-s_0) + \frac{4(1+r)}{\eta_0}\log\eta_0 - 4 \\ &-\frac{1}{(1-r)^2}\left[(6-21r+3r^2) + 2\eta_0(1+3r) + \frac{(1-r^2)(1-s_0)-\eta_0(1+r)}{\eta_0^2}\right. \\ &\left. -2\eta_0^2 - 2(2-r)(1-r)(1+\log\eta_0) + \eta_0(1-r)(1+2\log\eta_0)\right] \quad .\end{aligned} \tag{40}$$

The functions Ω_1' and Ω_2' denote the derivatives with respect to s_0 of the functions Ω_1 and Ω_2, which are given in eqs. (34) and (35). The exponentiated photon energy spectrum is now calculated using the following expression:

$$\frac{d\Gamma}{dx_\gamma} = \frac{d\Gamma_F}{dx_\gamma} + \Theta(x_{crit}-1)\frac{d\Gamma_7}{dx_\gamma} + \Theta(1-x_{crit})\frac{d\Gamma_7^{exp}}{dx_\gamma} \tag{41}$$

where x_{crit} defines, as before, the kinematic point used for the exponentiated version. One could use either this form or the earlier one given in Eq. (29) for the photon energy spectrum in the case $b \to s+\gamma+g$, with care taken to include the appropriate CKM factors. However, it turns out that numerically the two exponentiation procedures are very similar and lead to only small differences in the x_γ-distribution in the decays $B \to X_s+\gamma$. These differences are shown in Fig. 3 after the incorporation of the wave function effects, whose discussion is taken up next.

2.5 Energy-Momentum Profile of Inclusive Radiative Rare B-Decays

To get the physical profile of the final states, one has to incorporate the B-meson wave function effects on the partonic distributions discussed so far. These effects can at best be estimated in a model. However, one could fix the model parameters from independent data such as the lepton energy spectra in the CC semileptonic decays of the B-hadrons. A simple

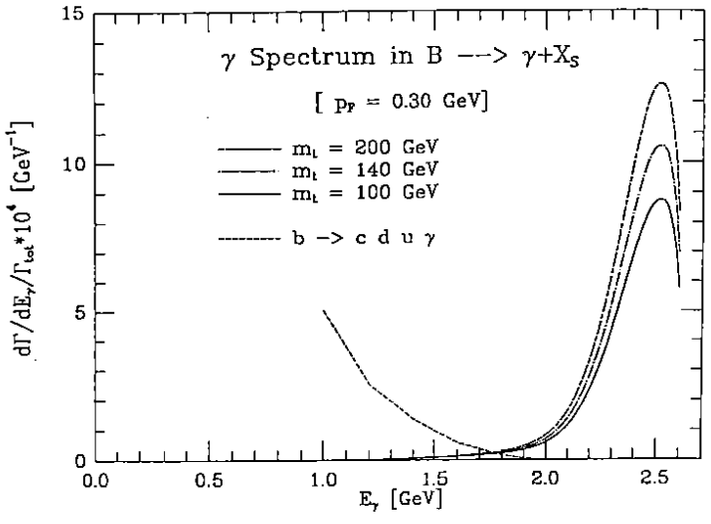

Figure 4: Inclusive photon energy spectrum for the process $B \to X_s + \gamma$ using perturbative QCD and the B-meson wave function model described in the text, with the parameter p_F set to 0.3 GeV and three representative values of the top quark mass, as indicated. The dashed curve corresponds to the photon energy spectrum from the background process $B \to X_c + \gamma$ (from [43]).

model used in [50,51] to implement the D- and B-meson bound state effects on the inclusive lepton energy spectra was employed in [39] to calculate the wave function effects on the photon energy and hadron mass spectra in the decays $B \to X_s + \gamma$. The corresponding distributions for the decay $B \to X_d + \gamma$ were calculated in [44]. Recapitulating briefly, the b-quark in this model is given a non-zero momentum (due to its being bound in the B-hadron) having a Gaussian distribution:

$$\phi(p) = \frac{4}{\sqrt{\pi} {p_F}^3} \exp(\frac{-p^2}{{p_F}^2}) \quad ; \quad p = |\vec{p}| \tag{42}$$

The energy-momentum constraint is imposed in the form:

$$W^2 = {M_B}^2 + {m_q}^2 - 2M_B\sqrt{p^2 + {m_q}^2} \tag{43}$$

where M_B is the B-meson mass, W, the effective mass of the b-quark, and m_q, the mass of the spectator quark in the B-meson, $B = b\bar{q}$. There are two important parameters that influence the shape of the spectra, namely W and p_F, which have been experimentally constrained to be: 0.21 $GeV \leq p_F \leq 0.39$ GeV and $W \simeq 5.0$ GeV, using the CLEO [52] and ARGUS analysis [53]). The other parameters used in the numerical calculations are $m_c = 1.68$ GeV, $m_s = 0.5$ GeV, and $m_u = m_d = 0$, though the small variation due to the uncertainty in the charmed quark mass will be displayed later.

We first show the dependence of the inclusive photon energy spectrum in the decay $B \to X_s + \gamma$ on the assumed exponentiated forms discussed in the previous section. Using for

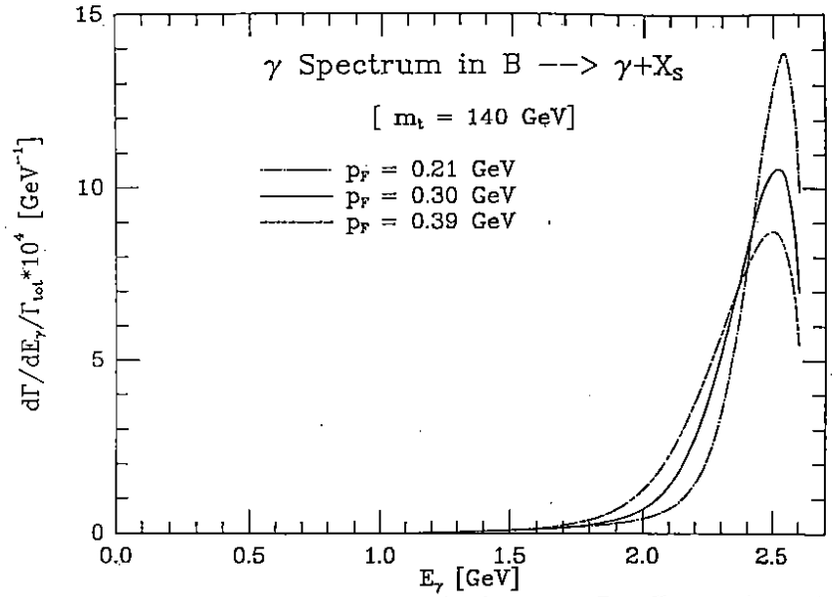

Figure 5: Inclusive photon energy spectrum for the process $B \to X_s + \gamma$ using perturbative QCD and the B-meson wave function model described in the text, and $m_t = 140$ GeV. The three indicated values of the parameter p_F bracket the recent $(\pm 1\sigma)$–fits of the CLEO data from the lepton energy spectrum in B-decays (from [39]).

the sake of definiteness the values $m_t = 140$ GeV and $p_F = 0.30$ GeV, the resulting spectra are displayed in Fig. 3. The two spectra are very similar; that is good since it implies that the ambiguity in the exponentiation procedure for the case $r \neq 0$ does not overly compromise theoretical predictivity. The dependence of the photon energy spectrum on the parameters m_t and p_F in the inclusive decays $B \to X_s + \gamma$ is shown in Figs. 4 and 5, respectively.

We note that the shape of the spectrum is not very sensitive to m_t (though the rate shows more sensitivity). This can be attributed to the wave function effects which don't depend on m_t and dominate for large x_γ, overpowering the m_t-dependence of the perturbative QCD contribution. An estimate of the photon energy spectrum from the background processes $B \to X_c + \gamma$ computed in ref. [54] using the quark decay, $b \to c + d + \bar{u} + \gamma$, can also be seen in Fig. 4. A clear separation between the background $(B \to X_c + \gamma)$ and signal $(B \to X_s + \gamma)$ is obtained for energetic photons having energy in excess of the kinematically allowed maximum for the indicated background process, $E_\gamma = (m_B^2 - m_{D^*}^2)/2m_B \simeq 2.0$ GeV.

As we already discussed, the inclusive photon energy spectrum for the decay $B \to X_d + \gamma$ depends on the CKM parameters ρ and η. This spectrum is shown in Fig. 6 for $m_t = 140$ GeV and $(\rho, \eta) = (0.4, 0.4)$, which corresponds to a point in the middle of the allowed (ρ, η) region in Fig. 7 (see below), obtained by incorporating all the available constraints on the CKM matrix elements. Comparing Figs. 5 and 6, it is clear that apart from their end-points, which differ numerically due to the differing thresholds in $B \to X_d + \gamma$ and $B \to X_s + \gamma$, the two spectra are very similar in shape. In view of this it will not be possible to disentangle the CKM suppressed decays $B \to X_d + \gamma$ from the dominant decays $B \to X_s + \gamma$ using the photon

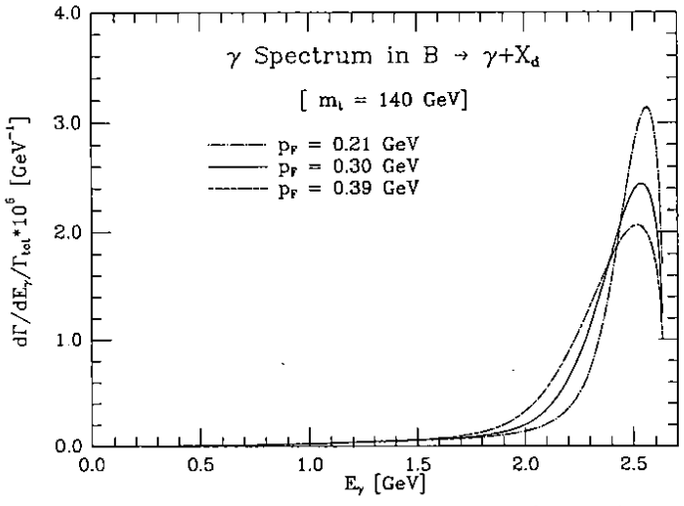

Figure 6: Inclusive photon energy spectrum for the process $B \to X_d + \gamma$ using perturbative QCD and the B-meson wave function model described in the text, with the indicated values of the parameter p_F and $m_t = 140$ GeV. In addition, we have set $\rho = 0.4$, $\eta = 0.4$ (from [44]).

spectral shapes alone. To distinguish the two inclusive decays from each other, one will have to flavour-tag the hadrons recoiling against the photon. The suppressed decays $B \to X_d + \gamma$ will involve non-strange hadrons, like $\pi\pi, \rho, A_1, ...$, as opposed to the CKM-allowed rare decays $B \to X_s + \gamma$, involving hadrons with the overall strangeness quantum number $S = -1$, like $K^*, K\pi, K^{**}, ...$ We hope that dedicated experiments in future B-facilities will have good particle identification to enable this separation.

The calculation for the inclusive photon spectra also yields the invariant mass distribution of the hadrons recoiling against the photon in the processes $B \to X_s + \gamma$, and $B \to X_d + \gamma$. These distributions are fairly broad (with the full width at half maximum $\simeq 1\ GeV$), and they peak broadly around the recoil hadron mass $(m_{X_s}, m_{X_d}) = (1.2 - 1.5)$ GeV, depending on the details of the B-meson wave functions. This feature could be interpreted as a statement that the decays $B \to X_s + \gamma$ and $B \to X_d + \gamma$ are expected to be dominated by the appropriate multibody final states, with no single resonance dominating. In view of the large phase space available in these decays, this is reasonable. In particular, it is very unlikely that the low mass states like $K^*\gamma$ and $\rho\gamma$ are substantial fractions of their respective inclusive branching ratios. The virtue of using the inclusive photon spectrum in radiative rare B-decay searches is two-fold. First, there is no suppression due to the branching ratio in any specific channel. second, and more importantly, this would enable a direct comparison of theory and experiment. On the less optimistic side, one should freely admit that such inclusive measurement would be an experimental feat!

2.6 Estimates of the Inclusive Branching Ratios $BR(B \to X_s + \gamma)$ and $BR(B \to X_d + \gamma)$

The results for the branching ratio $BR(B \to X_s + \gamma)$, obtained in the RG-improved effecive Hamiltonian approach and including the leading real and virtual corrections are shown as a function of the top quark mass in Fig. 1. The dependence of the branching ratio on the charm quark mass in the range 1.3 GeV $\leq m_c \leq$ 1.7 GeV is indicated by the error bars. Comparison of this result with the leading order QCD improved results for the two-body decay $b \to s + \gamma$ in Fig. 1 shows that the additional corrections lower the previously discussed estimates of the inclusive branching ratio $BR(B \to X_s + \gamma)$ by about 15 % across the top quark mass range. To quote a number from the next-to-leading order calculation we note that $BR(B \to X_s + \gamma) = 3.5 \times 10^{-4}$ for $m_t = 140$ GeV, and it rises to about 4.5×10^{-4} for $m_t = 250\ GeV$. Taking into account all the uncertainties, a firm prediction for the FCNC inclusive radiative B-decay in the Standard Model is:

$$BR(B \to X_s + \gamma) = (3 - 5) \times 10^{-4} \tag{44}$$

We now calculate the branching ratio for the CKM-suppressed inclusive decay $B \to X_d + \gamma$. Note that due to the contribution of the operator O_2 in $b \to d + g + \gamma$ the dependence of the rate on the CKM matrix-elements does not factorize any longer. This dependence can be written explicitly as [44]:

$$BR(B \to X_d + \gamma) = D_1 |\xi_t|^2 \left\{ 1 - \frac{1-\rho}{(1-\rho)^2 + \eta^2} D_2 - \frac{\eta}{(1-\rho)^2 + \eta^2} D_3 + \frac{D_4}{(1-\rho)^2 + \eta^2} \right\} , \tag{45}$$

where the coefficients D_i do not depend on the CKM matrix. Their m_t dependence is shown in Table 1 (for $m_c = 1.68$ GeV, $m_b = 5$ GeV, $m_d = 0$, $\alpha_s = 0.23$, $A = 0.926$ and $\lambda = 0.220$). As

$m_t(GeV)$	D_1	D_2	D_3	D_4
100	0.15	0.21	0.04	0.14
120	0.17	0.20	0.04	0.13
140	0.18	0.18	0.04	0.12
160	0.19	0.17	0.04	0.11
180	0.20	0.17	0.03	0.10
200	0.21	0.16	0.03	0.10

Table 1: Values of the coefficients D_i entering in Eq. (45) as a function of m_t (from [44]).

can be seen from the entries in Table 1, the coefficients $D_1, ..., D_4$ are not very sensitive to m_t. Also, while D_1, D_2, and D_4 are approximately similar and typically $O(0.15)$, the coefficient D_3 multiplying the CP-violating phase η is a lot smaller, being typically ~ 0.03. This implies that the CP-asymmetry both in the shape and normalization in the CKM-suppressed decay $B \to X_d + \gamma$, while formally of $O(\eta/((1-\rho)^2 + \eta^2))$ is numerically small due to the small coefficient D_3. Again, we shall not give any numbers for this. To get the inclusive branching ratio as a function of m_t, one has to vary the CKM parameters ρ and η over the presently

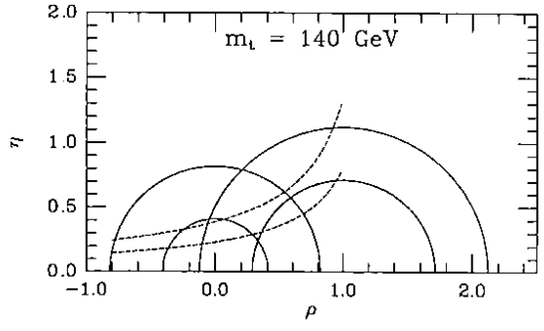

Figure 7: Constraints on the CKM parameters (ρ, η) from x_d, $|\epsilon|$ and $|V_{ub}|/|V_{cb}|$ measurements, as discussed in the text (from [44]).

allowed range. For this purpose one could use the following experimental inputs [13,15]:

$$\left|\frac{V_{ub}}{V_{cb}}\right| = 0.14 \pm 0.05 \tag{46}$$

$$|\epsilon| = (2.26 \pm 0.02) \times 10^{-3} \tag{47}$$

$$x_d = 0.67 \pm 0.10 \tag{48}$$

While the bounds on the ratio $\left|\frac{V_{ub}}{V_{cb}}\right|$ give directly $\sqrt{\rho^2+\eta^2}$, one has to take into account the m_t-dependence of $|\epsilon|$ and x_d as well as specify other phenomenological parameters needed in their analysis. We use the following expressions for $|\epsilon|$ [55]:

$$\begin{aligned} |\epsilon| \;=\; & \frac{G_F^2 f_K^2 m_K m_W^2}{6\sqrt{2}\pi^2 \Delta m_K} B_K \left(A^2\lambda^6\eta\right) \{x_c\,(\eta_{ct} f_3(x_c, x_t) - \eta_{cc}) \\ & + \eta_{tt}\, x_t\, f_2(x_t)\, A^2\lambda^4(1-\rho)\Big\} \end{aligned} \tag{49}$$

Here, the η_i are QCD correction factors, $\eta_{cc} \simeq 0.85$, $\eta_{tt} \simeq 0.61$, $\eta_{ct} \simeq 0.36$ for $\Lambda_{QCD} = 200$ MeV [56], $m_K = 498$ MeV, $\Delta m_K = 3.5 \cdot 10^{-12}$ MeV, $f_K = 160$ MeV, $x_i \equiv m_i^2/M_W^2$, and the functions f_2 and f_3 are given by

$$\begin{aligned} f_2(x) &= \frac{1}{4} + \frac{9}{4}\frac{1}{(1-x)} - \frac{3}{2}\frac{1}{(1-x)^2} - \frac{3}{2}\frac{x^2 \ln x}{(1-x)^3} \\ f_3(x,y) &= \ln\frac{y}{x} - \frac{3y}{4(1-y)}\left(1 + \frac{y}{1-y}\ln y\right) . \end{aligned} \tag{50}$$

The final parameter in the expression for $|\epsilon|$ is B_K, which represents our ignorance of the matrix element $\langle K^0|(\bar{d}\gamma^\mu(1-\gamma_5)s)^2|\overline{K^0}\rangle$. We shall take $B_K = 2/3 \pm 1/6$. This leads to the two hyperbolae in Fig. 7.

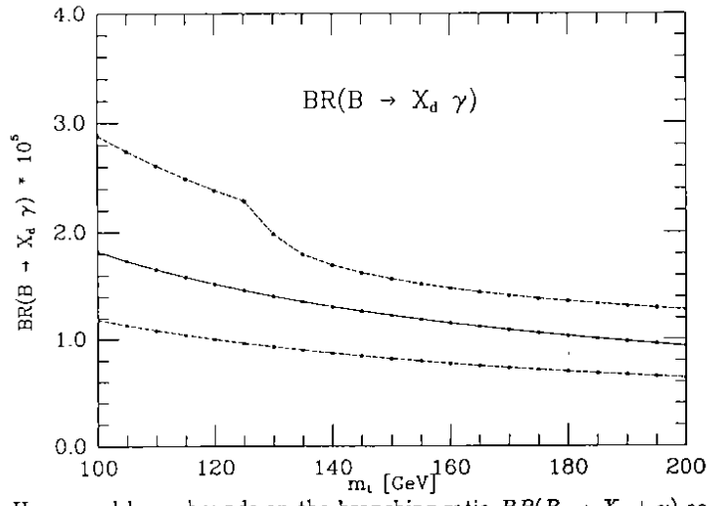

Figure 8: Upper and lower bounds on the branching ratio $BR(B \to X_d + \gamma)$ as a function of m_t, obtained by varying over the allowed range in the (ρ, η) plane, using the constraints from Fig. 7. The full curve corresponds to $x_d = 0.67$ (from [44]).

We now turn to B_d^0-$\overline{B_d^0}$ mixing, which is dominated by the t-quark exchange:

$$x_d \equiv \frac{(\Delta m)_B}{\Gamma} = \tau_B \frac{G_F^2}{6\pi^2} m_W^2 m_B \left(f_{B_d}^2 B_{B_d}\right) \eta_B x_t f_2(x_t) |\xi_t|^2 . \tag{51}$$

Here, η_B is the QCD correction for which we take $\eta_B = 0.85$, and assume $f_B\sqrt{B_B} = (0.20 \pm 0.03)$GeV, as suggested by recent Lattice simulations [57]. In addition, we use $\tau_B = 1.18 \times 10^{-12}$ sec and $m_B = 5.277$ GeV [13]. The constraints from x_d leads to the two semi-circles centered at $(\rho, \eta) = (1, 0)$ shown in Fig. 7.

The resulting branching ratio $BR(B \to X_d + \gamma)$ is shown in Fig. 8 as a function of m_t. Taking into account the present uncertainties in ρ, η, and m_t, it has been estimated in [44] that the inclusive rate for the CKM-suppressed radiative decay in the SM is:

$$BR(B \to X_d + \gamma) = (0.5 - 3) \times 10^{-5} \tag{52}$$

We remark in passing that the ratio of the inclusive decay widths $\Gamma(B \to X_d + \gamma)/\Gamma(B \to X_s + \gamma)$ is less dependent on m_t and hence a better measure of the CKM parameters ρ and η.

2.7 Estimates of $BR(B \to K^* + \gamma)$ and $BR(B \to \rho + \gamma)$

Having the hadronic invariant mass distributions for the decays $B \to X_d + \gamma$ and $B \to X_s + \gamma$, it is tempting to estimate the exclusive branching ratios for the lowest lying resonances using the assumption of vector meson dominance in the low-mass part of the spectrum. The motivation of doing this comes from experimental studies in semileptonic D-decays, in which the hadronic mass spectrum in the range $m_K + m_\pi \le m_{X_s} \le 1.0$ GeV is found to be completely saturated by the K^*-resonance [16,17]. To estimate the branching ratio $BR(B \to K^* + \gamma)$

from the inclusive rate for $B \to X_s + \gamma$, we assume that also here the K^* dominates in the same mass range. Although analogous information from the CKM-suppressed decays $D \to X_d \ell \nu_\ell$ and $B \to X_u \ell \nu_\ell$ is still not at hand, it is reasonable to assume that in the mass range between $2m_\pi \leq m(X_d) \leq 1.0$ GeV, the decays $B \to X_d + \gamma$ will be dominated by the ρ-resonance. Using this intuitive argument, one could integrate the spectrum in the decays $B \to X_d + \gamma$ in the indicated range to estimate the branching ratio for $B \to \rho + \gamma$. The branching ratio $BR(B \to K^* + \gamma)$ so obtained is given in Table 2, where the values of m_t and p_F are indicated. As noted earlier, there is no CKM-matrix element dependence in this branching ratio. Taking into account the uncertainty on m_t and p_F, one estimates [39,44]:

$$BR(B \to K^* + \gamma) = (3 - 8) \times 10^{-5} \quad . \tag{53}$$

The best experimental bound on this branching ratio is due to CLEO [58], $BR(B \to K^* + \gamma) < (9.2) \times 10^{-5}$ @(90% $C.L.$). Based on our estimates, we conclude that the discovery of the first rare B-decay mode is just around the corner!

$m_t(GeV) =$	100	140	200
$p_F = 0.21\ GeV$	5.4	6.5	7.8
$p_F = 0.30\ GeV$	3.9	4.8	5.7
$p_F = 0.39\ GeV$	3.1	3.8	4.5

Table 2: Branching Ratio for the decay $B \to K^* + \gamma$ in units of 10^{-5} (from [44]).

The branching ratio for the decay $B \to \rho + \gamma$ for m_t between 100 and 200 GeV and the indicated values of the parameter p_F is shown in Table 3, where the entries again correspond to the central values in Fig. 7, namely $\rho = \eta = 0.4$. It turns out that to a precision better

$m_t(GeV) =$	100	140	200
$p_F = 0.21\ GeV$	2.1	2.5	3.0
$p_F = 0.30\ GeV$	1.6	1.9	2.2
$p_F = 0.39\ GeV$	1.3	1.5	1.8

Table 3: Branching Ratio for the decay $B \to \rho + \gamma$ in units of $(10^{-6} \times |V_{td}|^2/5.06 \cdot 10^{-5})$ (from [44]).

than 1% this branching ratio depends on ρ and η only through the combination $|\xi_t|^2/|V_{bc}|^2 = \lambda^2[(1-\rho)^2 + \eta^2]$. The reason for this is not too difficult to understand. The inclusive photon spectrum near $E_\gamma \simeq E_\gamma^{\max}$, where the photon in the two-body decay $B \to \rho + \gamma$ is to be found, is dominated by the magnetic moment operator O_7 which depends only on $|\xi_t|$, as can be seen from the effective Hamiltonian for $b \to d + \gamma + (g)$. The following branching ratio has been estimated in [44]:

$$BR(B \to \rho + \gamma) = (1 - 3) \times 10^{-6} \times \frac{|V_{td}|^2}{5.06 \times 10^{-5}} \quad , \tag{54}$$

Since the dependence on the CKM matrix-element has been made explicit, the uncertainty indicated in the above branching ratio reflects the dependence on the parameters m_t and p_F. A much firm prediction is however obtained on the relative rates for the decays $B \to \rho + \gamma$ and $B \to K^* + \gamma$ from which both the m_t-dependence, as well as, the dependence on the details of the B-meson wave-function (here characterized by the parameter p_F) drops out, giving [44]:

$$\frac{\Gamma(B \to \rho + \gamma)}{\Gamma(B \to K^* + \gamma)} = 0.04 \times \frac{|V_{td}|^2}{5.06 \times 10^{-5}} \tag{55}$$

In view of this, the indicated exclusive rare decays are very well suited for determiming the CKM matrix element, $|V_{td}|$.

3 FCNC B-DECAYS INVOLVING DILEPTONS

In this section, we review the calculations for the FCNC inclusive semileptonic B-decays, $b \to (s,d) + \ell\bar{\ell}$ $(\ell = e, \mu, \nu)$, and in doing this will treat the quark states synonymous with the corresponding hadron states. These decays have also been studied quite extensively in the context of SM, as well as, non-SM scenarios. Compared to the rare radiative B-decays considered in the previous section, the FCNC semileptonic B-decays $b \to (s,d) + \ell^+\ell^-$ $(\ell = e, \mu)$ receive very significant contributions from the so-called long-distance processes. For the dominant decays $b \to s + \ell^+\ell^-$ $(\ell = e, \mu)$, these contributions are dominated by the decays $B \to (J/\psi, \psi')X \to \ell^+\ell^- X$, which have been measured by the ARGUS and CLEO collaborations [13], giving a branching ratio $O(10^{-3})$. One would naively think of subtracting this background by removing the dileptons having an invariant mass close to the J/ψ and ψ' resonances. However, as the corresponding short distance contribution is estimated to be $O(10^{-6})$ for the decays $b \to s + \ell^+\ell^-$ $(\ell = e, \mu)$, the long distance contribution is overwhelming and it influences the spectrum also in regions away from the J/ψ and ψ' resonances. Hence, one has to treat the long- and short-distance contributions coherently. We follow here closely the calculations reported in [40], whose sign convention agrees with the choice in [34,42], leading to a constructive interference in the invariant dilepton mass distribution. Inclusive decay rates involving the dielectron and dimuon final states are reported and various distributions sensitive to m_t are shown. At the end of this section we discuss the rates for the FCNC B-decays involving a pair of neutrini, $b \to (s,d) + \nu\bar{\nu}$. With hermetic detectors and sufficient statistics, this final state may be detected in LEP experiments.

3.1 FCNC B-Decays $B \to (X_s, X_d) + \ell^+\ell^-$

The effective Hamiltonian for the rare decays $b \to (s,d) + \ell\bar{\ell}$ $(\ell = e, \mu, \nu)$ is derived as before by integrating out the top quark and the W-bosons. We shall concentrate here on the CKM-allowed decays $b \to s + \ell\bar{\ell}$ $(\ell = e, \mu, \nu)$, but most of what is being said here also applies (with obvious modifications) to the case $b \to d + \ell\bar{\ell}$ $(\ell = e, \mu, \nu)$. Also, since already the lowest order processes $b \to (s,d) + \ell\bar{\ell}$ $(\ell = e, \mu, \nu)$ provide a non-trivial lepton-energy and mass-spectra, we shall not consider real gluon bremsstrahlung corrections. This is motivated by the $O(\alpha_s)$ corrections to the rate and spectra in the analogous CC semileptonic decays $b \to (c,u)\ell\nu_\ell$, which lead to at most $O(20\%)$ effects in the decay rates and leave the normalized distributions stable [50,51]. The renormalization group improvements effected in terms of the

Wilson coefficients are, however, included in presenting the rates and distributions being discussed.

In the approximation of keeping only dimension-6 operators, the appropriate basis for the FCNC B-decays involving dileptons consists of twelve operators and the effective Hamiltonian may be written as

$$H_{eff}(b \to s + \ \ell^+\ell^- \ (\ell = e, \mu)) = -\frac{4G_F}{\sqrt{2}}\lambda_t \sum_{j=1}^{12} \tilde{C}_j(\mu)\tilde{O}_j(\mu) \tag{56}$$

Detailed considerations, however, show that the coefficients of some of the operators and their mixing with the remaining ones are small and the basis may be truncated. The operators of interest in the present context are, $\tilde{O}_1, \tilde{O}_2, \tilde{O}_7, \tilde{O}_8$ and $\tilde{O}_9$. The first three in this list were given in the previous section while discussing the decays $b \to s + \gamma + g$. Since the operators $\tilde{O}_j$ are used to calculate the matrix elements for the transition $b \to s+$(virtual) photon, we have to take a one loop matrix element of the operators $\tilde{O}_1, \tilde{O}_2$, and $\tilde{O}_7$. The remaining operators are defined below:

$$\tilde{O}_8 = \frac{\alpha}{4\pi}(\bar{s}\gamma_\mu L b)(\bar{\ell}\gamma_\mu \ell) \tag{57}$$

$$\tilde{O}_9 = \frac{\alpha}{4\pi}(\bar{s}\gamma_\mu L b)(\bar{\ell}\gamma_\mu\gamma_5 \ell) \tag{58}$$

and the Wilson coefficients are [35,34]

$$C_8(m_b) = C_8(M_W) + \frac{4\pi}{\alpha_s(M_W)}\left[\frac{4}{33}\left(1-\eta^{-11/23}\right) - \frac{8}{87}\left(1-\eta^{-29/23}\right)\right] \tag{59}$$

$$C_9(m_b) = C_9(M_W) \tag{60}$$

where we have dropped the tilde on the coefficients $\tilde{C}_i$ for ease of writing. To avoid possible mix-up in the notation, we point out that the operator $\tilde{O}_8$ in the effective Hamiltonian here and the operator $\hat{O}_8$ in the corresponding Hamiltonian for $b \to s + \gamma + g$ are different operators, hence also the Wilson coefficients C_8 in the two cases are different. Again, the large logarithms of the type $\ln(M_W^2/m_b^2)$ are included in the Wilson coefficients and not in the matrix elements of the operators.

The coefficients $C_8(m_W)$ and $C_9(m_W)$ appearing above can be written in terms of three functions B, C and D, following [34,35].

$$C_8(M_W) = \frac{1}{\sin^2\theta_W}B(x) + \frac{-1+4\sin\theta_W}{\sin^2\theta_W}C(x) + D(x) + \frac{4}{9} \tag{61}$$

$$C_9(M_W) = \frac{-1}{\sin^2\theta_W}B(x) + \frac{1}{\sin^2\theta_W}C(x) \tag{62}$$

with

$$B(x) = \frac{1}{4}\left[\frac{x}{x-1} - \frac{x}{(x-1)^2}\ln x\right] \tag{63}$$

$$C(x) = \frac{x}{4}\left[\frac{-x/2+3}{x-1} - \frac{3x/2+1}{(x-1)^2}\ln x\right] \tag{64}$$

$$D(x) = \left[\frac{19x^3/36 - 25x^2/36}{(x-1)^3} + \frac{x^4/6 - 5x^3/3 + 3x^2 - 16x/9 + 4/9}{(x-1)^4}\ln x\right] \tag{65}$$

The matrix-element for the process of interest can be written as:

$$\mathcal{M}(b \to s + \ell^+\ell^-) = 2\sqrt{2}\,G_F \frac{\alpha}{sin^2\,\theta_W}\lambda_t \frac{-1}{4\pi}\overline{\mathcal{M}} \tag{66}$$

where we have again dropped the small terms due to the intermediate u-quark, and have used the CKM unitarity constraint to relate $\lambda_c \equiv V_{cb}V_{cs}^*$ to λ_t. The reduced matrix element $\overline{\mathcal{M}}$ can be shown to be:

$$\overline{\mathcal{M}} = C_{\mathcal{A}}\,\bar{s_L}\gamma_\mu b_L\,\bar{\ell_L}\gamma^\mu\ell_L + C_{\mathcal{B}}\,\bar{s_L}\gamma_\mu b_L\,\bar{\ell_R}\gamma^\mu\ell_R + 2\sin^2\theta_W C_7(\mu)\bar{s}i\sigma_{\mu\nu}q^\nu/q^2(m_s L + m_b R)b\,\bar{\ell}\gamma_\mu\ell \tag{67}$$

As pointed out earlier, one has to calculate both the long- and short-distance contribution to $\overline{\mathcal{M}}$. We concentrate first on the short distance piece and give the long distance contribution later. The functions $C_{\mathcal{A}}$, $C_{\mathcal{B}}$ are given by:

$$C_{\mathcal{A}} = \sin^2\theta_W(-C_8(m_b) + C_9(m_b) - (3C_1(m_b) + C_2(m_b))g(m_c/m_b, q^2)) \tag{68}$$

$$C_{\mathcal{B}} = \sin^2\theta_W(-C_8(m_b) - C_9(m_b) - (3C_1(m_b) + C_2(m_b))g(m_c/m_b, q^2)) \tag{69}$$

and the function $g(m_c/m_b, q^2)$ arises from the one-loop matrix element of the four-quark operators [34,35]:

$$g(m_c/m_b, y) = -\left\{\frac{4}{9}\ln\left(\frac{m_c^2}{m_b^2}\right) - \frac{8}{27} - \frac{16}{9}\frac{m_c^2}{y} + \frac{2}{9}\sqrt{\left|1-\frac{4m_c^2}{y}\right|}\left(2+\frac{4m_c^2}{y}\right)R(y)\right\} \tag{70}$$

with

$$R(y) = \ln\left|\frac{1+\sqrt{1-\frac{4m_c^2}{y}}}{1-\sqrt{1-\frac{4m_c^2}{y}}}\right| + i\pi \text{ for } y > 4m_c^2 \tag{71}$$

$$R(y) = 2\arctan\left(\frac{1}{\sqrt{1-\frac{4m_c^2}{y}}}\right) \text{ for } y < 4m_c^2 \tag{72}$$

The invariant dilepton mass distribution in the inclusive decays can now be calculated easily with the help of the matrix elements, given above. For the inclusive decay rate contribution from the short-distance piece, one estimates:

$$BR(B \to X_s + e^+e^-) = (1-2) \times 10^{-5}$$

and

$$BR(B \to X_s + \mu^+\mu^-) = (6-8) \times 10^{-6} \tag{73}$$

for the top quark mass range, 100 GeV $< m_t <$ 200 GeV. These estimates are to be contrasted with the recent upper limit for the (averaged) B-meson branching ratio from the UA1 collaboration: $BR(B \to X + \mu^+\mu^-) = 5 \times 10^{-5}$ [59], indicating that the present experimental sensitivity is an order of magnitude away in this channel. The branching ratios for the Cabibbo-suppressed FCNC decays $b \to d + \ \ell^+\ell^- \ (\ell = e, \mu)$ can be obtained by scaling the corresponding $b \to s + \ \ell^+\ell^- \ (\ell = e, \mu)$ rates by the CKM factor $(|V_{td}|/|V_{ts}|)^2$. The relative rates $BR(B \to X_d + \ell^+\ell^-)/BR(B \to X_s + \ell^+\ell^-)$ are independent of m_t and their eventual

measurement would determine the indicated CKM matrix-element ratio. While the precise value depends on the parameters, ρ and η, as discussed in the previous section, as an order of magnitude one expects a suppression by a factor $O(20)$ for the CKM-suppressed FCNC semileptonic decays in SM, yielding (for $m_t = 100 - 200$ GeV):

$$BR(B \to X_d + e^+e^-) = (0.5 - 1.0) \times 10^{-6}$$

and

$$BR(B \to X_d + \mu^+\mu^-) = (3 - 4) \times 10^{-7} \tag{74}$$

Some of these decay rates should be measurable at a first generation B-factory and in high energy hadronic collisions, such as at the Tevatron, LHC and SSC.

The calculations so far, however, take into account only the short distance contributions. In addition to this, there are long distance contributions from the intermediate $c\bar{c}$ state. Formally, this contribution can be implemented by the replacement of the function $g(m_c/m_b, q^2)$ by $G(m_c/m_b, q^2)$ in the expressions for C_A and C_B above[54 where [40],

$$G(m_c/m_b, q^2) = \{g(m_c/m_b, q^2) + \frac{3}{\alpha^2}\kappa \sum_{V_i=\Psi,\Psi'} \frac{\pi\Gamma[V_i \to l^+l^-]M_{V_i}}{M_{V_i}^2 - q^2 - iM_{V_i}\Gamma_{V_i}}\} \tag{75}$$

The pole contributions from the J/ψ and ψ' with the Breit-Wigner form are explicitly indicated.

It is well known that the Wilson coefficient sum $3C_1(m_b) + C_2(m_b)$ depends very sensitively on the QCD scale parameter Λ_{QCD}, as well as the renormalization point μ [60]. For instance, taking $\Lambda_{QCD} = 400$ MeV and the scale $\mu = m_b$ one has $3C_1(m_b) + C_2(m_b) = -0.17$, while for $\Lambda_{QCD} = 100$ MeV one obtains $3C_1(m_b) + C_2(m_b) = -0.41$, and for $\Lambda_{QCD} = 100$ MeV and using the renormalization point $\mu = 2m_b$ one finds $3C_1(2m_b) + C_2(2m_b) = -0.58$. Although the QCD corrected inclusive nonleptonic decay rate is stable against changes in Λ_{QCD}, the semi-inclusive channels $B \to J/\psi X_s$ and $B \to \psi' X_s$ have rather large rate uncertainties due to cancellations in the relevant combination of the Wilson coefficients. Since the leading order renormalization of the particular combination is very significant, in our opinion, higher order QCD corrections need to be calculated to estimate the semi-inclusive decay channels in question quantitatively. Though these calculations are now available [60], their impact on this particular decay branching ratio has not yet been fully worked out. We tentatively conclude that the long-distance contribution to the FCNC dilepton decay rates is not in quantitative rapport with the available QCD estimates.

A good strategy to calculate the inclusive dilepton invariant mass and related distributions in the decays $b \to s + \ell^+\ell^-$ ($\ell = e, \mu$), pending a satisfactory theoretical resolution of the long-distance puzzle in the decays $B \to (J/\psi, \psi')\ X_s$, is to use the data to calibrate the long-distance contribution. Using the branching ratios from the Particle Data Group [13] $BR(B \to J/\psi X \to l^+l^- X) = BR(B \to J/\psi X)BR(J/\psi \to l^+l^-) \simeq 7\times10^{-4}$ fixes the constant κ introduced in the resonance part of the amplitude for $b \to s\ell^+\ell^-$. Numerically, a value $\kappa(3C_1(m_b) + C_2(m_b)) = -1$ reproduces the data well. Curiously, this amounts to neglecting the QCD corrections in the decay $B \to (J/\psi, \psi')X_s$, since $3C_1(m_W) + C_2(m_W) = -1$. Fixing the normalization of the long distance piece from data, the relevant distributions and branching ratios can be obtained in a straight forward way. We show two such distributions here, namely the dilepton invariant mass and the forward-backward asymmetry of the charged l^+ -lepton in the rest frame of the dilepton pair. Defining the variable $z \equiv \cos\theta$, as the angle

between the momentum of the B-meson and that of l^+-lepton in the rest frame of the dilepton, the forward-backward asymmetry for a fixed invariant mass q^2 is obtained by integrating the double differential branching ratio ($\frac{d^2BR}{dq^2dz}$) with respect to the angular variable (z),

$$A(q^2) \equiv \frac{\int_0^1 dz \frac{d^2BR}{dq^2dz} - \int_{-1}^0 dz \frac{d^2BR}{dq^2dz}}{\int_0^1 dz \frac{d^2BR}{dq^2dz} + \int_{-1}^0 dz \frac{d^2BR}{dq^2dz}} \tag{76}$$

In the region where $A(q^2)$ is positive, the number of l^+ scattered in the forward hemisphere is more than the one in the backward hemisphere in the center of mass frame of the dilepton.

The asymmetry in the dilepton angular distribution can be qualitatively understood as follows. The decays $b \to s + \ell^+\ell^-$ ($\ell = e, \mu$) occur through γ , Z and W^+W^- exchange diagrams. For low m_t ($\frac{m_t}{M_W} < 1$) the photon contribution dominates and the vector-like interactions to the leptonic current remain substantial, consequently the asymmetry is small. However, for $\frac{m_t}{M_W} > 1$, the contribution from the Z-exchange diagrams becomes important and the coefficient of the left-handed leptonic current grows as m_t^2, leading to a large asymmetry. (A part of the coefficient for the vector current also behaves in the same way because Z also couples to the vector current.) It should be noted that the asymmetry depends on the invariant dilepton mass. At and near the J/ψ and ψ' peaks, the asymmetry is small since the resonances couple to the vector leptonic current.

3.2 Dilepton Invariant-mass and Asymmetry Distributions in $B \to (X_s, X_d) + \ell^+\ell^-$

Some results of interest taken from [40] are summarized in Figs. (9)-(11). In Fig. 9, we show the invariant dilepton mass distribution, $dBR/d\hat{s}$, for three assumed values of the top quark mass, $m_t = 100,\ 150,\ 200\ GeV$. Here, the variable $\hat{s}$ is the normalized dilepton invariant-mass, $\hat{s} = m_{ll}^2/m_b^2$. Away from the resonance regions, $m_{ll}^2 = m_{J/\psi,\psi'}^2$, the dilepton mass distribution is sensitive to the top quark mass. This can also be seen quantitatively in Table 4, where the branching ratios, integrated over well defined regions of the dilepton invariant mass in the decays $B \to X_s + \ell^+\ell^-$, with $\ell = e, \mu$, are shown. To get an information on the dynamics of the short distance component (and hence to gain sensitivity on m_t), it will be crucial to measure the dilepton mass spectra in the regions called (i), (iii), and (v) in Table 4. The double differential distribution $d^2BR/d\hat{s}dz|_{\hat{s}=0.3}$ is shown in Fig. 10

$m_t(GeV)$	(i)	(ii)	(iii)	(iv)	(v)
100	1.8×10^{-6}	6.8×10^{-4}	4.3×10^{-7}	3.3×10^{-5}	1.8×10^{-7}
150	2.7×10^{-6}	6.8×10^{-4}	6.6×10^{-7}	3.3×10^{-5}	4.1×10^{-7}
200	4.3×10^{-6}	6.8×10^{-4}	1.1×10^{-6}	3.3×10^{-5}	8.5×10^{-7}

Table 4: Branching ratio for the decay $B \to X_s + \ell^+\ell^-$ with $\ell = e, \mu$ in different regions of the dilepton invariant mass, $s = m_{ll}^2$. (i): 1.0 GeV$^2 \le s \le (M_{J/\Psi} - \delta)^2$, (ii): $(M_{J/\Psi} - \delta)^2 \le s \le (M_{J/\Psi} + \delta)^2$, (iii): $(M_{J/\Psi} + \delta)^2 \le s \le (M_{\Psi'} - \delta)^2$, (iv): $(M_{\Psi'} - \delta)^2 \le s \le (M_{\Psi'} + \delta)^2$, (v): $(M_{\Psi'} + \delta)^2 \le s \le (M_b - M_s)^2$, where an energy resolution of $\delta = 20$ MeV at the J/ψ and ψ' resonances has been assumed (from ref. [40]).

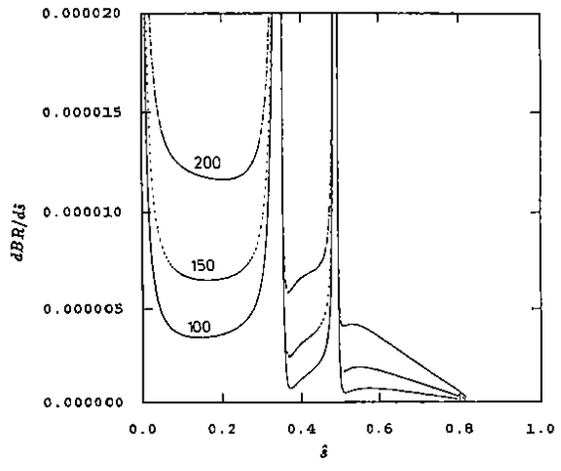

Figure 9: The differential branching ratio $dBR/d\hat{s}$ as a function of the scaled invariant dilepton mass $\hat{s} = s/m_b^2$ in the decay $b \to s + \ell^+\ell^-$ ($\ell = e, \mu$). Assumed top quark mass values are indicated on the curves (from ref. [40]).

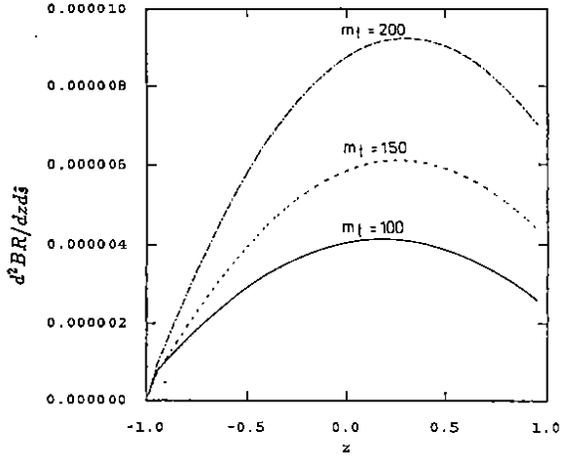

Figure 10: The angular distribution $d^2BR/dzd\hat{s}$ in the decay $b \to s + \ell^+\ell^-$ ($\ell = e, \mu$), for a fixed value of the scaled dilepton invariant mass $\hat{s} = 0.3$. The assumed top quark mass values $m_t = 100,\ 150,\ 200\ GeV$ are indicated on the curves. (from ref. [40]).

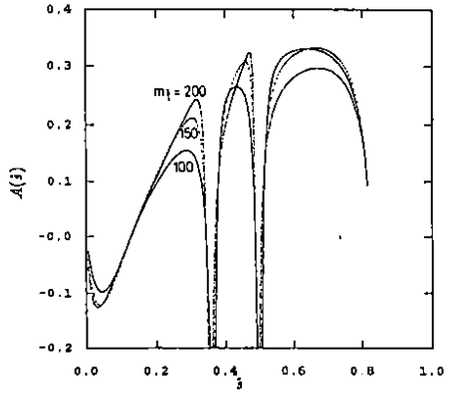

Figure 11: Forward-backward asymmetry of the dileptons in the decays $b \to s + \ell^+\ell^-$ ($\ell = e, \mu$), $A(\hat{s})$, as a function of the scaled invariant dilepton mass, $\hat{s}$, for the indicated values of the top quark mass (from ref. [40]).

for $m_t = 100,\ 150,\ 200$ GeV. Finally, in Fig. 11 we show the asymmetry for the decays $b \to s + \ell^+\ell^-$ ($\ell = e, \mu$), defined above, in three different invariant dilepton mass ranges for the assumed values of the top quark mass, $m_t = 100,\ 150,\ 200$ GeV.

3.3 Estimates of the FCNC B-Decays $B \to (X_s, X_d) + \nu\bar{\nu}$

As the final inclusive rare B-decays, we take up the FCNC B-decays involving two neutrini $b \to (s, d) + \nu\bar{\nu}$. The exclusive decays in this chain, involving for example $B \to (K, \pi)\nu\bar{\nu}$ and $B \to (K^*, \rho)\nu\bar{\nu}$, will be discussed in the next section. The FCNC dineutrino B-decays are experimentally very difficult to measure, except probably in a high luminosity LEP environment, involving the decay $Z^0 \to b\bar{b}$, where such events have a nice tag: large missing energy and momentum in a b-quark jet with no charged lepton. From the theoretical point of view, on the other hand, these decays are much simpler to deal with, since the operator basis given for $b \to s + \ell\bar{\ell}$ ($\ell = e, \mu, \nu$) reduces to only one operator, which is the difference of the $\hat{O}_8$ and $\bar{O}_9$ operators. Thus, a left handed current for the neutrino appears which couples pointlike to the left handed current of the $b \to s$ transition. The Wilson coefficient of this operator is D_9 [28]

$$D_9(M_W) = \frac{1}{\sin^2\theta_w}\left[\frac{1}{8}x + \frac{3}{8}\frac{x(x-2)}{(x-1)^2}\ln x + \frac{3}{8}\frac{x}{x-1}\right] \tag{77}$$

D_9, like C_9, is not affected by the QCD scaling corrections. This gives

$$H_{eff}(b \to s + \nu\bar{\nu}) = -\frac{8G_F}{\sqrt{2}}V_{tb}V_{ts}^* D_9(M_W)\left(\frac{\alpha}{4\pi}\right)(\bar{s}\gamma_\mu Lb)(\bar{\nu}\gamma_\mu L\nu) \tag{78}$$

The differential distribution in the missing invariant mass for the inclusive decay $b \to s + \nu\bar{\nu}$ are given in [41], together with the corresponding distributions for some exclusive decays. The branching ratios for the inclusive decays $B \to X_s + \nu\bar{\nu}$, summed over three neutrino species, and $m_t = 150$ GeV, has been estimated as [41]:

$$BR(B \to X_s + \nu\bar{\nu}) = (6.5) \times 10^{-5} \tag{79}$$

Again, for the CKM-suppressed inclusive decays $b \to d + \nu\bar{\nu}$, one expects:

$$\frac{BR(B \to X_d + \nu\bar{\nu})}{BR(B \to X_s + \nu\bar{\nu})} = \frac{|V_{td}|^2}{|V_{ts}|^2} \tag{80}$$

and as an order of magnitude one estimates this ratio to be $O(0.05)$.

4 EXCLUSIVE RARE B-DECAYS

To predict the exclusive decay rates one has to face the non-trivial problem of evaluating the hadronic matrix elements of the effective operators, which we have evaded so far! Clearly, using a non-perturbative model there is no problem in estimating the exclusive decays and various model dependent approaches have been developed along these lines [30,31,32,39], of which we discussed one in the preceding sections. It may eventually be possible to sandwitch the various effective operators discussed earlier between definite states relevant for B-decays and evaluate their matrix elements in the lattice QCD framework. While this approach has the promise of reducing an inherent ambiguity in the comparison of experiment and theory, there are hardly any definitive results available concerning rare B-decays from lattice simulations.

As mentioned in the introduction, the HQET approach is also promising in the quantitative studies of B-decays. In particular, concerning rare B-decays, it has been remarked by Isgur and Wise [22] that if one considers only the upper (dominant) components of the b-quark field, one could relate some of the form factors appearing in the exclusive rare B-decays, such as $B \to K^* + \gamma$, to the ones in the CC semileptonic decays, such as $B \to \rho\ell\nu_\ell$. On the other hand, one could argue that since the momentum transfer in the decay $B \to K^* + \gamma$ is large, typically $O(m_B/2)$, there may be substantial hard perturbative corrections to the Isgur-Wise relations, apart from the obvious power corrections. It has, however, been noticed in ref. [24] that the hard perturbative corrections in the decays being discussed obey the Isgur-Wise relations obtained in the static limit. An interesting result has been obtained in ref. [24], relating the decay rate $B \to K^* + \gamma$ to the CC semileptonic decay $B \to \rho + \ell + \nu_\ell$ at a point in the Dalitz plot $d^2\Gamma/dE_\rho dE_l$ which corresponds to the maximum recoil. This allows, in principle, a direct experimental comparison when enough data on both the decays in question become available. The magnitude of the perturbative form factors is still somewhat debatable.

We review some of the results obtained in the HQET approach for the rare decays $B \to K^*\gamma$ and $B \to (K, K^*)\ell\bar{\ell}$ ($\ell = e, \mu, \nu$). They have been obtained in the approximation of treating both the b- and s-quark as heavy, since in this approximation one could relate the rare B-decays with the semileptonic decays of the D- and B-mesons. As the s-quark is not heavy, corrections in powers of(Λ/m_s) need to be included in order to obtain reliable results. This programme is still to be carried out. Despite this, it is tempting to use the static limit to predict the absolute rare B-decay rates. The results discussed in this section are not rigorous and they should be considered as just another estimate.

4.1 Hadronic Matrix Elements in the HQET Approach

We briefly introduce the formalism that has been employed in ref. [41] for calculating the matrix elements that appear in a number of exclusive rare B-decays. For this purpose we

introduce the bilinear operators involving heavy quarks, which are generically denoted as:

$$\bar{h}'_{v'} \Gamma h_v \tag{81}$$

where Γ denotes some combination of the Dirac gamma matrices and v and v' are the velocities of the heavy quarks of type h and h'. It is known that all the matrix elements of this type of operators are described in terms of a single universal function ξ, the so called Isgur-Wise function [20], which depends only on the product of the two velocities $v \cdot v'$. One could use the trace formalism given in [21] to evaluate the matrix elements. In this formalism the heavy 0^- mesons H moving with some velocity v are described by the matrices

$$H(v) = \frac{1}{2}\sqrt{m_H}\gamma_5(\not{v} - 1) \tag{82}$$

while the matrices for the corresponding 1^- states are given by

$$H^*(v, \epsilon) = \frac{1}{2}\sqrt{m_H}\not{\epsilon}(\not{v} - 1) \tag{83}$$

where ϵ is the polarization vector of the 1^- state. The matrix element of the operators (81) are then given by (for example for $1^- \to 1^-$ transitions):

$$< H'^{(*)}(v', \epsilon')|\, \bar{h}'_{v'} \Gamma h_v \,|H^{(*)}(v, \epsilon) >= \xi(v \cdot v')\ \mathrm{Tr}\ \left\{H'^{(*)}(v', \epsilon')\Gamma H^{(*)}(v, \epsilon)\right\} \tag{84}$$

In the heavy quark limit, one could relate the rare B decays to the semileptonic decays of the D- and B-mesons, since all these decays are described by the same function. As mentioned earlier, a better reference process to calculate the decay rate for $B \to K^* + \gamma$ is the decay $B \to \rho\ell\nu_\ell$. However, not having the benefit of data in this mode, the Isgur-Wise function has been constrained by using data on the semileptonic decays of the D-meson, namely $D \to K\ell\nu_\ell$ and $D \to K^*\ell\nu_\ell$. In ref. [41] two different parametrizations of the Isgur-Wise function have been used; the first one is a monopole form:

$$\xi(v \cdot v') = \frac{w_0^2}{w_0^2 - 2 + 2v \cdot v'} \tag{85}$$

and the second one is encountered in models employing wave functions to calculate the decay form factors:

$$\xi(v \cdot v') = \exp\left(\beta(1 - v \cdot v')\right) \tag{86}$$

Data on the decay $D \to K\ell\nu_\ell$ have been used to fit w_0 in (85) and β in (86). The best fit is obtained for $w_0 \approx 1.80$ and $\beta \approx 0.5$. We shall use theses parametrizations for all the decay modes discussed below.

4.2 Decay Rate for $B \to K^*\gamma$

For the decay $B \to K^*\gamma$ only the operator O_7 from the list given in section 2 contributes.

$$< K^*\gamma|H_{eff}|B >= -\frac{4G_F}{\sqrt{2}} V_{tb}V_{ts}^* C_7(m_b) < K^*\gamma|\hat{O}_7(m_b)|B > \tag{87}$$

The hadronic matrix element needed for (87) is now evaluated in the heavy quark limit for the b- and s-quarks. It is thus given in terms of the Isgur-Wise function. In the heavy

quark limit the operator $\hat{O}_7$ simplifies. The derivative from the field strength gives a factor $q = m_B v - m_K v'$ and, since in the heavy quark limit $\not{v}' s = s$ and $\not{v} b = b$, one has

$$\bar{s}\sigma^{\mu\nu}(1+\gamma_5)bq^\nu = -m_B\bar{s}\gamma_\mu(1-\gamma_5)b - m_B\bar{s}\gamma_\mu(1+\gamma_5)b + q_\mu\bar{s}(1+\gamma_5)b \tag{88}$$

The hadronic matrix elements are:

$$< K^*(v',\epsilon)|\bar{s}\gamma_\mu(1\mp\gamma_5)b|B(v) >= \sqrt{m_{K^*}m_B}\xi(v\cdot v')\left((1+v\cdot v')\epsilon_\mu - v'_\mu(\epsilon\cdot v) \pm i\varepsilon_{\mu\alpha\beta\gamma}v^\alpha v'^\beta\epsilon^\gamma\right) \tag{89}$$

$$< K^*(v',\epsilon)|\bar{s}(1+\gamma_5)b|B(v) >= \sqrt{m_{K^*}m_B}\xi(v\cdot v')(\epsilon\cdot v) \tag{90}$$

This then leads to the following decay rate:

$$\begin{aligned}\Gamma(B\to K^*\gamma) &= \frac{1}{16\pi^4}G_F^2\alpha|\xi(v\cdot v')|^2|V_{tb}|^2|V_{ts}|^2|C_7(m_B)|^2 \\ &\quad\times(k\cdot v)^3 m_B^2\frac{m_{K^*}}{m_B}\left(1+\frac{m_B}{m_{K^*}}\right)^2\end{aligned} \tag{91}$$

where the Isgur-Wise function is evaluated at the point

$$v\cdot v' = \frac{1}{2m_Bm_{K^*}}(m_B^2+m_{K^*}^2) \approx 3.04 \tag{92}$$

This value is far outside the kinematic range of the semileptonic D-decays; the maximum value of $v\cdot v'$ in $D\to Ke\nu$ and $D\to K^*e\nu$ is $v\cdot v'\approx 2.01$ and $v\cdot v'\approx 1.29$, respectively. In fact this large extrapolation makes the prediction of the decay rate $\Gamma(B\to K^*+\gamma)$ particularly prone to the assumed parametrizations of the Isgur-Wise function. Defining the exclusive to inclusive decay rate ratio :

$$R(B\to K^*\gamma) \equiv \frac{\Gamma(B\to K^*\gamma)}{\Gamma(B\to X_s\gamma)} \tag{93}$$

one could express this ratio in a compact form [41]:

$$R(B\to K^*\gamma) = \frac{m_{K^*}}{4m_B}|\xi(v\cdot v')|^2\left(1+\frac{m_B}{m_{K^*}}\right)^2 \tag{94}$$

Where for the sake of getting analytic results, we have used the QCD corrected $b\to s\gamma$ rate discussed earlier to estimate $\Gamma(B\to X_s\gamma)$

$$\Gamma(B\to X_s\gamma) = \frac{G_F^2}{4\pi^4}\alpha|V_{tb}|^2|V_{ts}|^2|C_7(m_B)|^2(k\cdot v)^3m_B^2 \tag{95}$$

Table 5 contains the predictions for the total rate (given for $m_t = 100$ GeV), the branching fractions and the ratio $R(B\to K^*\gamma)$ for the two assumed parametrizations of the Isgur-Wise function, obtained in ref. [41]. The dependence of the exclusive decay rate on m_t, and hence of the branching fraction, is the same as the one given for the inclusive branching ratio in Fig. 1 since, in the approximation being used, they are given by the same function $C_7(m_B)$. The exclusive to inclusive ratio R is obviously independent of m_t. It should be noted here that the dependence of the decay rate on the parameter w_0 of the monopole parametrization is quite strong. For instance, using the value $w_0 = 1.1$ as obtained from a fit to the decay spectrum of $B\to D^*e\nu$ [23] gives a rather small value for R, $R = 9\%$, whereas the fit to

the semileptonic D decays does not depend significantly on w_0. The reason for this strong dependence of the $B\to K^*\gamma$ decay rate lies in the already mentioned extrapolation of the Isgur-Wise function. Hence, we expect the uncertainties to be largest for this rare decay and we must conclude that the branching ratio $BR(B\to K^*\gamma)$ in the heavy quark approach can at present be determined to only within a factor 4.

The branching ratio $BR(B\to K^*\gamma)$ and the ratio $R(B\to K^*\gamma)$ obtained here can be compared with the calculations of the corresponding quantities presented in section 2, which were based on the estimates of refs. [39,44]. We recall that these estimates gave $BR(B\to K^*\gamma) = (3-6)\times 10^{-5}$ and $R(B\to K^*\gamma) = (10-18)\%$. The authors of ref. [31] obtained $R(B\to K^*\gamma) = 15\%$, based on QCD sum rules supplemented by a pole model. We note that the branching ratios for $B\to K^*\gamma$ obtained in the HQET limit, with the mentioned parametrizations, are significantly larger.

	Eq.(85), $w_0 = 1.80$	Eq.(86), $\beta = 0.50$
$\Gamma(B\to K^*\gamma)$ (GeV)	$8.3\cdot 10^{-17}$	$6.1\cdot 10^{-17}$
$BR(B\to K^*\gamma)$	$1.5\cdot 10^{-4}$	$1.1\cdot 10^{-4}$
$R(B\to K^*\gamma)$	40 %	28 %

Table 5: Decay rates and branching ratios for the decay $B\to K^*\gamma$, for $m_t = 100$ GeV (from ref. [41]).

4.3 Decay Rates for $B\to K\ell^+\ell^-$, $B\to K^*\ell^+\ell^-$

As discussed at some length in the last section, one expects a significant long-distance contribution in the exclusive FCNC dilepton decays as well from the intermediate states $B\to J/\psi(K,K^*)\to \ell^+\ell^-(K,K^*)$. In particular, the resulting interference pattern in the invariant dilepton mass distributions is very important. We shall not present the invariant dilepton mass distributions for exclusive decays and concentrate only on the rates from the short-distance contribution. We recall that also in these decays all the five operators given in section 3 for the inclusive decays $b\to s+\ \ell^+\ell^-$ $(\ell = e,\mu)$ are relevant. The contributions of $\tilde{O}_1,\tilde{O}_2$ and $\tilde{O}_7$ are via a one-loop diagram which renders the invariant mass spectrum of the lepton pair nontrivial. Their contribution may be written as [41]:

$$\begin{aligned}\tilde{O}_1 &= 3\tilde{O}_2 \\ &= (\bar{s}\gamma_\mu(1+\gamma_5)b)\left(\bar{l}\gamma_\mu l\right)g(m_{ll}^2)\end{aligned} \tag{96}$$

where m_{ll}^2 denotes the invariant mass of the lepton pair and the function $g(m_c/m_b,y)$ has been given before.

The hadronic matrix elements are evaluated as before in terms of the Isgur-Wise function and are given by:

$$< K(v')|\bar{s}\gamma_\mu(1\mp\gamma_5)b|B(v) > = \sqrt{m_Km_B}\xi(v\cdot v')(v_\mu+v'_\mu) \tag{97}$$

$$< K(v')|\bar{s}(1+\gamma_5)b|B(v) > = \sqrt{m_Km_B}\xi(v\cdot v')(1+v\cdot v') \tag{98}$$

$$< K^*(v',\epsilon)|\bar{s}\gamma_\mu(1\mp\gamma_5)b|B(v) > = \sqrt{m_{K^*}m_B}\xi(v\cdot v') \times\left((1+v\cdot v')\epsilon_\mu - v'_\mu(\epsilon\cdot v)\pm i\varepsilon_{\mu\alpha\beta\gamma}v^\alpha v'^\beta\epsilon^\gamma\right) \quad (99)$$

$$< K^*(v',\epsilon)|\bar{s}(1+\gamma_5)b|B(v) > = \sqrt{m_{K^*}m_B}\xi(v\cdot v')(\epsilon\cdot v) \quad (100)$$

Incorporating this in the the effective Hamiltonian, the following invariant dilepton mass differential rates have been derived in [40], which should be used in regions away from the J/ψ and ψ' resonances.

$$\frac{d\Gamma}{dm_{ll}^2}(B\to K\ell^+\ell^-) = \frac{G_F^2m_B^3}{(2\pi)^3}|V_{tb}V_{ts}^*|^2\frac{1}{48r}\left(\frac{\alpha}{4\pi}\right)^2(Q_+Q_-)^{3/2}(1+r)^2\xi^2(v\cdot v') \times\left[\left|C_{8eff}(m_{ll}^2,m_b)+\frac{2}{1+r}C_7(m_B)\right|^2+|C_9(m_B)|^2\right] \quad (101)$$

$$\frac{d\Gamma^*}{dm_{ll}^2}(B\to K^*\ell^+\ell^-) = \frac{G_F^2m_B^3}{(2\pi)^3}|V_{tb}V_{ts}^*|^2\frac{1}{48r}\left(\frac{\alpha}{4\pi}\right)^2Q_+\sqrt{Q_+Q_-}\xi^2(v\cdot v') \times\left[\left(\left|C_{8eff}(m_{ll}^2,m_b)\right|^2+|C_9(m_B)|^2\right)\left(4\hat{x}^2(1+r^2-\hat{x}^2)+Q_+(1-r)^2\right) +4\left|C_7(m_b)\right|^2\left(\frac{4}{\hat{x}^2}((1-r^2)^2-\hat{x}^2)+Q_+\right) +16\mathrm{Re}\left(C_7(m_b)C_{8eff}(m_{ll}^2,m_b)\right)(1-r^2-\hat{x}^2)\right] \quad (102)$$

and the various abbreviations are defined as:

$$C_{8eff}(m_{ll}^2,m_B) = C_8(m_B)+(3C_1(m_B)+C_2(m_B))\,g(m_{ll}^2) \quad (103)$$

$$\hat{x}^2=\frac{m_{ll}^2}{m_B^2} \qquad r=\frac{m_{K(*)}}{m_B} \quad (104)$$

$$Q_\pm = (1\pm r)^2-\hat{x}^2 \quad (105)$$

$$v\cdot v' = \frac{1}{2r}(1+r^2-\hat{x}^2) \quad (106)$$

Integrating the differential distributions given above, the decay rates for $m_t = 100$ GeV are given in Table 6 and 7 for the two assumed parametrizations of the Isgur-Wise function. Note that the differential rate for $B\to K^*e^+e^-$ becomes singular for $\hat{x}\to 0$ and thus the total rate will depend logarithmically on the kinematic lower bound, namely $4m_l^2/m_B^2$. The rate for $B\to Ke^+e^-$ does not become singular in this limit, and thus the difference between the rates for $B\to Ke^+e^-$ and $B\to K\mu^+\mu^-$ is negligible.

Tables 6 and 7 also show the ratio R, defined analogously to the ratio $R(B\to K^*\gamma)$ previously, for the indicated exclusive decays, with the inclusive rate for $B\to X_s ee$ and $B\to X_s\mu\mu$ discussed earlier. The numbers in Tables 6 and 7 are in agreement with the corresponding estimates in refs. [31,32,34]. We remark that the branching ratios given in the tables above, which are calculated for $m_t = 100\ GeV$, are enhanced by approximately a factor of 2.0, 2.5, and 3.0, for the decays $b\to s\ell^+\ell^-$, $B\to K^*\ell^+\ell^-$, and $B\to K\ell^+\ell^-$, respectively, for $m_t = 200\ GeV$. The exclusive to inclusive decay rate ratios, R, are however, very stable against the variation of m_t.

4.4 Decay Rates for $B\to K\nu\bar{\nu}$ and $B\to K^*\nu\bar{\nu}$

These processes, like their inclusive counterparts discussed in the preceding section, are theoretically simpler to deal with since the operator basis given in section 2 reduces to only one

	Eq.(85), $w_0 = 1.80$	Eq.(86), $\beta = 0.50$
$\Gamma(B\to K\ell^+\ell^-)$ (GeV)	$1.4\cdot10^{-19}$	$6.3\cdot10^{-20}$
$BR(B\to K\ell^+\ell^-)$	$2.5\cdot10^{-7}$	$1.1\cdot10^{-7}$
$R(B\to Ke^+e^-)$	4%	2%
$R(B\to K\mu^+\mu^-)$	7%	3%

Table 6: Decay rates, branching fractions and the ratios R for the decays, $B\to K\ell^+\ell^-$ with $\ell = e,\mu$ ($m_t = 100GeV$) (from ref. [41]).

	Eq.(85), $w_0 = 1.80$	Eq.(86), $\beta = 0.50$
$\Gamma(B\to K^*e^+e^-)$ (GeV)	$1.3\cdot10^{-18}$	$9.6\cdot10^{-19}$
$BR(B\to K^*e^+e^-)$	$2.3\cdot10^{-6}$	$1.7\cdot10^{-6}$
$R(B\to K^*e^+e^-)$	35%	27%
$\Gamma(B\to K^*\mu^+\mu^-)$ (GeV)	$6.7\cdot10^{-19}$	$5.7\cdot10^{-19}$
$BR(B\to K^*\mu^+\mu^-)$	$1.2\cdot10^{-6}$	$1.0\cdot10^{-6}$
$R(B\to K^*\mu^+\mu^-)$	35%	26%

Table 7: Decay rates, branching fractions and the ratios R for the decays $B\to K^*e^+e^-$ and $B\to K^*\mu^+\mu^-$ ($m_t = 100GeV$) (from ref. [41]).

operator. The effective Hamiltonian and the Wilson coefficient of this operator have already been given earlier. The hadronic matrix elements can again be related to the single Isgur-Wise function. The differential distribution in the missing invariant mass, for three neutrino generations, can be written as [41]:

$$\frac{d\Gamma}{dm_{\nu\nu}^2}(B\to K\nu\bar{\nu}) = \frac{G_F^2m_B^3}{(2\pi)^3}|V_{tb}V_{ts}^*|^2\left(\frac{\alpha}{4\pi}\right)^2\frac{1}{8r}((Q_+Q_-)^{3/2} (1+r)^2\xi^2(v\cdot v')\,|D_9(M_W)|^2 \quad (107)$$

$$\frac{d\Gamma^*}{dm_{\nu\nu}^2}(B\to K^*\nu\bar{\nu}) = \frac{G_F^2m_B^3}{(2\pi)^3}|V_{tb}V_{ts}^*|^2\left(\frac{\alpha}{4\pi}\right)^2\frac{1}{8r}Q_+\sqrt{Q_+Q_-}\xi^2(v\cdot v')\,|D_9(M_W)|^2 \left(4\hat{m}^2(1+r^2-\hat{m}^2)+Q_+(1-r^2)\right) \quad (108)$$

These distributions can be seen in [41], where the invariant missing mass spectra have been calculated using Eq. (85) with $w_0 = 1.80$ as a parametrization of the Isgur-Wise function.

The decay rates, branching fractions and the ratio R for the decays $B\to(K,K^*)\nu\bar{\nu}$ summed over three generations can be seen in Table 8.

Concerning the CKM suppressed FCNC decays, such as $B\to(\pi,\rho)\ \ell^+\ell^-$ and the ones involving the neutrino pair $B\to(\pi,\rho)\ \nu\bar{\nu}$, we note that they are related to the corresponding CKM-allowed decays, discussed above. The ratios of the corresponding CKM-suppressed and -allowed exclusive decays rates are expected to be down by the same CKM-factor that we discussed in the preceding sections for the relative rate $\Gamma(B\to\rho+\gamma)/\Gamma(K^*+\gamma)$. All such ratios are good measures of the CKM matrix-element $|V_{td}|$. The particular simplicity of the

	Eq. (85), $w_0 = 1.80$	Eq. (86), $\beta = 0.50$
$\Gamma(B \to K\nu\bar{\nu})$ /GeV	$1.3 \cdot 10^{-18}$	$5.8 \cdot 10^{-19}$
$BR(B \to K\nu\bar{\nu})$	$2.3 \cdot 10^{-6}$	$1.0 \cdot 10^{-6}$
$R(B \to K\nu\bar{\nu})$	8%	4%
$\Gamma(B \to K^*\nu\bar{\nu})$ /GeV	$4.7 \cdot 10^{-18}$	$4.3 \cdot 10^{-18}$
$BR(B \to K^*\nu\bar{\nu})$	$8.2 \cdot 10^{-6}$	$7.5 \cdot 10^{-6}$
$R(B \to K^*\nu\bar{\nu})$	30%	28%

Table 8: Decay rates, branching fractions and the ratios R for the decays $B \to K\nu\bar{\nu}$ and $B \to K^*\nu\bar{\nu}$ ($m_t = 100GeV$) (from ref. [41]).

exclusive decays $B \to (K, K^*, \pi, \rho)\ \nu\bar{\nu}$ and their relations with the CC semileptonic B-decays has also been noted by Deshpande and collaborators.

4.5 Decay Rates for $B_s^0 \to \ell^+\ell^-$ and $B_s^0 \to \gamma\ \gamma$

These decays were discussed some time ago in ref. [61] in the lowest (1 loop) order. With the help of the effective Hamiltonian formalism developed since then, it is easy to show that the decay rates don't get renormalized by QCD effects, and one has:

$$\Gamma(B_s^0 \to \tau^+\tau^-) = \frac{G_F^2}{2\pi}(\frac{\alpha}{4\pi})^2 f_B^2 m_B m_\tau^2 \sqrt{1 - \frac{4m_\tau^2}{m_B^2}} |V_{tb}V_{ts}^*|^2 |C_9(m_W)|^2 \qquad (109)$$

Here f_B is the B-meson pseudoscalar coupling constant for which we assume $f_B = 200\ MeV$, and numerically $C_9(m_W) = 3.73$ for $m_t = 150\ GeV$. The branching ratio for $B_s^0 \to \ell^+\ell^-$ can be written as

$$BR(B_s^0 \to \tau^+\tau^-) = 1.8 \times 10^{-7}(\frac{f_B(GeV)}{0.2})^2(\frac{|C_9(m_W)|}{3.73})^2 \qquad (110)$$

The rates for the decays $B_s^0 \to \mu^+\mu^-$ and $B_s^0 \to e^+e^-$ are suppressed compared to the corresponding rate for $\tau^+\tau^-$ by $(m_\mu/m_\tau)^2$ and $(m_e/m_\tau)^2$, respectively, and they are indeed very small, as can be seen in Table 9. Again, one can express the decay rates $\Gamma(B_d^0 \to \ell^+\ell^-)$ in terms of the rates for $\Gamma(B_s^0 \to \ell^+\ell^-)$ using the relation in the CKM model: $\frac{\Gamma(B_d^0 \to \ell^+\ell^-)}{\Gamma(B_s^0 \to \ell^+\ell^-)} = \frac{|V_{td}|^2}{|V_{ts}|^2}(1+\delta)$, with δ an $SU(3)$-breaking parameter. Since the present unitarity bound on the CKM ratio is $\frac{|V_{td}|^2}{|V_{ts}|^2} \leq 0.16$, one expects the branching ratios for $B_d^0 \to \ell^+\ell^-$ to be suppressed by $O(0.05)$ compared to the corresponding decays $B_s^0 \to \ell^+\ell^-$, given in table 9.

Finally, the branching ratio for the process $B_s^0 \to \gamma\ \gamma$ is:

$$BR(B_s^0 \to \gamma\gamma) = 1.5 \times 10^{-8}(\frac{f_B(GeV)}{0.2})^2(\frac{|I^+(m_t)|}{0.43})^2 \qquad (111)$$

where the function $I^+(m_t)$ is given in ref. [61]. The presently available bounds from experimental searches are also listed in Table 9.

Decay Modes	Br	Experimental Upper Limits (90 % C.L.)
$(B_d, B_u) \to X_s\gamma$	4.2×10^{-4}	8.4×10^{-4} [CLEO][58]
$(B_d, B_u) \to K^*\gamma$	$(4.0 - 7.0) \times 10^{-5}$	0.92×10^{-4} [CLEO][58]
$(B_d, B_u) \to X_d\gamma$	$(0.5 - 3.0) \times 10^{-5}$	–
$(B_d, B_u) \to \rho + \gamma$	$(1.0 - 3.0) \times 10^{-6}$	–
$(B_d, B_u) \to X_s e^+e^-$	1.2×10^{-5}	–
$(B_d, B_u) \to X_s\mu^+\mu^-$	6.7×10^{-6}	5.0×10^{-5} [UA1][59]
$(B_d, B_u) \to Ke^+e^-$	4.4×10^{-7}	5.0×10^{-5} [PDG][13]
$(B_d, B_u) \to K\mu^+\mu^-$	4.4×10^{-7}	1.5×10^{-4} [PDG][13]
$(B_d, B_u) \to K^*e^+e^-$	3.7×10^{-6}	–
$(B_d, B_u) \to K^*\mu^+\mu^-$	2.3×10^{-6}	2.3×10^{-5} [UA1][59]
$(B_d, B_u) \to X_s\nu\bar{\nu}$	6.6×10^{-5}	–
$(B_d, B_u) \to K\nu\bar{\nu}$	5.2×10^{-6}	–
$(B_d, B_u) \to K^*\nu\bar{\nu}$	2.0×10^{-5}	–
$B_s \to \gamma\gamma$	2.0×10^{-8}	–
$B_s \to \tau^+\tau^-$	1.8×10^{-7}	–
$B_s \to \mu^+\mu^-$	8.3×10^{-10}	–
$B_s \to e^+e^-$	2.0×10^{-14}	–

Table 9: Estimates of the branching fractions for FCNC B-decays in the Standard Model for $m_t = 150\ GeV$ and $f_B = 200\ MeV$. Note that the CKM-suppressed decays, given in row 3 and 4, depend on $|V_{td}|$, and the numbers correspond to $|V_{td}| = 0.007$. Experimental upper limits are also listed.

5 OVERVIEW and OULOOK

The theoretical interest in rare B-decays lies in the first place in their potential role as precision tests of the Standard Model in the flavour sector. Within the Standard Model, their eventual measurements will provide quantitative information about the top quark mass and more importantly about the CKM matrix-elements, V_{td}, V_{ts} and V_{tb}. In particular, the CKM-suppressed rare B-decays directly measure V_{td}. However, rare B-decay may provide one of the early hints for the non-SM physics. It is, therefore, imperative to get as reliable estimates of these decays in the SM as possible.

We have discussed in this report a number of inclusive and exclusive branching ratios and distributions involving rare B-decays in the Standard Model. The estimates presented here are based on the applications of QCD, whose role lies in both sharpening the theoretical expectations and in providing a dependable energy-momentum profile of the final states. Based on the successful applications of perturbative QCD in studies of the inclusive CC semileptonic and non-leptonic B-decays, it is fair to expect that applications of the same in inclusive FCNC B-decays will also provide reliable estimates.

In view of this, we emphasize that it would be worthwhile to attempt measurements of the hard photon spectra in the inclusive rare B-decays, $B \to X_s + \gamma$ and $B \to X_d + \gamma$. Such hard photons ($E_\gamma > 2.0$ GeV in the B-meson rest frame) are not present in the backgrond

CC B-decays due to kinematics. In principle, one could distinguish the CKM-allowed and -suppressed rare B-decays by flavour-tagging the hadrons in X_s, which should have an overall strangeness quantum number $S = -1$, and in X_d, consisting of light hadrons with an overall $S = 0$.

Theoretical predictivity in exclusive rare B-decays is less sharp. This is so since rare B-decays involve the so-called heavy to light quark transitions, as opposed to the CC decays $B \to (D, D^*)\ell\nu_\ell$, which have been quantitatively studied in the HQET framework and are under theoretical control. Significantly firm statements on the exclusive rare B-decays can be made if the CKM-suppressed CC exclusive decays become available experimentally. From an experimental point of view, however, exclusive rare B-decay searches, such as $B \to K^* + \gamma$, $B \to \rho + \gamma$, and $B \to (K, K^*, \pi, \rho)\ \ell^+\ell^-$, are easier given enough statistics. In view of the ongoing seraches, we reviewed estimates of some exclusive decays. They were in part based on vector meson dominance approximation, which we consider experimantally motivated in similar circumstances, and in the HQET approach. Estimates presented here and in the literature lead us to believe that the first of the CKM-allowed radiative rare B-decays is waiting in the wings for its discovery!

While the radiative rare B-decays are expected to have larger branching ratios, and hence emphasized quite a bit here, the FCNC B-decays involving dileptons are equally promising, since they can be searched for in hadron collisions also, such as at the Fermilab Tevatron, LHC, and SSC. With an estimated yield of $O(10^{10} - 10^{12})$ B-hadrons at these facilities, many of the inclusive and exclusive dilepton decay modes are detectable.

Acknowledgemets :

A good part of these lectures is based on work done in collaboration with Christoph Greub, Thomas Mannel, and Takuya Morozumi. I would like to thank them for this collaborative effort which I have enjoyed thoroughly. The help of Thomas Mannel and Christoph Zecher in the preparation of this manuscript is gratefully acknowledged. This work has been partially supported by the International Centre for Theoretical Physics, Trieste, Staff Associate Programme.

6 References

[1] S.L. Glashow, Nucl. Phys. **22** (1961) 579; S. Weinberg, Phys. Rev. Lett. **19** (1967) 1264; A. Salam, in *Elementary Particle Theory*, Editor: N. Svartholm (Almqvist and Wiksell) (1968).

[2] M. Kobayashi and K. Maskawa, Prog. Theor. Phys. **49** (1973) 652.

[3] N. Cabibbo, Phys. Rev. Lett. **10** (1963) 531.

[4] S.L. Glashow, J. Illiopoulos, and L. Maiani, Phys. Rev. **D2** (1970) 1285.

[5] S.W. Herb et al. (CFS Collaboration), Phys. Rev. Lett. **39** (1977) 252.

[6] W.R. Innes et al. (CFS Collaboration), Phys. Rev. Lett. **39** (1977) 1240.

[7] K. Ueno et al. (CFS Collaboration), Phys. Rev. Lett. **42** (1979) 486.

[8] Ch. Berger et al. (PLUTO Collaboration), Phys. Lett. **76B** (1978) 243.

[9] C. W. Darden et al. (DASP II Collaboration), Phys. Lett. **76B** (1978) 246.

[10] J. K. Bienlein et al. (DESY-Heidelberg Collaboration) Phys. Lett. **78B** (1978) 360; C. W. Darden et al. (DASP II Collaboration), Phys. Lett. **78B** (1978) 364.

[11] D. Andrews et al. (CLEO Collaboration), Phys. Rev. Lett. **44** (1980) 1108.

[12] T. Böhringer et al. (CUSB Collaboration), Phys. Rev. Lett. **44** (1980) 1111.

[13] J.J. Hernández et al. (Particle Data Group), Phys. Lett. **B 239** (1990) 1.

[14] B-Decays, Editor: S. Stone (World Scientific, Singapore, 1992).

[15] H. Schröder, in ref. [14].

[16] J.C. Anjos et al. (E691 Collaboration), Phys. Rev. Lett. **62** (1989) 1587 and FERMILAB PUB-90/124-E.

[17] M. Adamovich et al. (WA82 Collaboration), CERN/PPE 91-99 (1991).

[18] K. Kodama et al. (E653 Collaboration), Phys. Lett. **B274** (1992) 246.

[19] H. Politzer and M. Wise, Phys. Lett. **B206** (1988) 681; *ibid* **B208** (1988) 504; M. Voloshin and M. Shifman, Sov. J. Nucl. Phys. **45** (1987) 292; *ibid* **47** (1988) 511; E. Eichten and B. Hill, Phys. Lett. **B234** (1990) 511; H. Georgi, Phys. Lett. **B240** (1990) 447; B. Grinstein, Nucl. Phys. **B339** (1990) 253.

[20] N. Isgur and M. Wise, Phys. Lett. **B232** (1989) 113; *ibid* **B237** (1990) 527.

[21] H. Georgi, B. Grinstein and M. Wise, Phys. Lett. **B252** (1990) 456; A.F. Falk et al., Nucl. Phys.**B343** (1990) 1. A. Falk, B. Grinstein and M. Luke Preprint HUTP-90/A044 (1990).

[22] N. Isgur and M. Wise, Phys. Rev. **D42** (1990) 2388.

[23] T. Mannel *Heavy Quark Effective Theory*, Habilitationsschrift, Technische Hochschule Darmstadt, IKDA 92/6 (1992).

[24] G. Burdman, J.F. Donoghue, Phys. Lett. **B270** (1991) 55.

[25] B.A. Campbell and P.J. O'Donnell, Phys. Rev. **D25**(1982) 1989.

[26] S. Bertolini, F. Borzumati and A. Masiero, Phys. Rev. Lett. **59**(1987) 180.

[27] N.G. Deshpande et al., Phys. Rev. Lett. **59**(1987) 183.

[28] W. Hou, R. Willey and A. Soni, Phys. Rev. Lett. **58** (1987) 1608.

[29] R. Grigjanis et al., Phys. Lett. **B213**(1988) 355.

[30] T. Altomari, Phys. Rev. **D37** (1988) 677

[31] C. Dominguez, N. Paver and Riazuddin, Phys. Lett. **B214** (1988) 459.

[32] N.G. Deshpande, Preprint OITS 413 (1989).

[33] B. Grinstein, M. J. Savage and M. B. Wise, Nucl. Phys. **B319** (1989) 271.

[34] C.S. Lim, T. Morozumi and A.I. Sanda, Phys. Lett. **B218** (1989) 343.

[35] B. Grinstein, R. Springer and M. B. Wise, Nucl. Phys. **B339** (1990) 269.

[36] G. Cella et al., Phys. Lett. **248B** (1990) 181.

[37] M. Misiak, Phys. Lett. **B269** (1991) 161.

[38] A. Ali and C. Greub , Z. Phys. **C49** (1991) 431.

[39] A. Ali and C. Greub , Phys. Lett. **B259** (1991) 182.

[40] A. Ali, T. Mannel, and T. Morozumi, Phys. Lett. **273B** (1991) 505.

[41] A. Ali and T. Mannel, Phys. Lett. **B649** (1991) 447; E **274** (1992) 526.

[42] P.J.O'Donnell and H.K.K. Tung, Phys. Rev. **D43** (1991) R2067;
N. Paver and Riazuddin, ICTP Trieste Report(1991).

[43] A. Ali, DESY Report 91-080 (1991). (To be published in Proc. of First Int. A.D. Sakharov Conf. on Physics, Lebedev Inst., Moscow (1991).)

[44] A. Ali and C. Greub , DESY Report 92-048 (1992).

[45] S. Bertolini, F. Borzumati and A. Masiero, in ref. [14].

[46] L. Wolfenstein, Phys. Rev. Lett. **51** (1983) 1945.

[47] T. Inami and C.S. Lim, Progr. Theor. Phys. **65**(1981) 297.

[48] P. Cho and B. Grinstein, Harvard Univ. Report HUTP-91/A020(1991).

[49] J.M. Soares, Carnegie Mellon Report CMU-HEP91-03 (1991).

[50] A. Ali and E. Pietarinen, Nucl. Phys. **B154**(1979) 519.

[51] G. Altarelli et al., Nucl. Phys. **B208**(1982) 365.

[52] R. Fulton et al. (CLEO), Phys. Rev. Lett. **64** (1990) 16;
S. Stone (Private communication).

[53] H. Albrecht et al. (ARGUS Collaboration), Phys. Lett. **B234** (1990) 409; DESY Report, DESY 90-088(1990).

[54] G. Eilam et al., Univ. of Western Ontario Report (1990).

[55] A.J. Buras, W. Słominski and H. Steger, Nucl. Phys. **B238** (1984) 529; **B245** (1984) 369.

[56] J. Flynn, Mod. Phys. Lett. **A5** (1990) 877.

[57] M. Lusignoli et al. Univ. di Roma Preprint n.810 (1991);
C. Alexandrou et al., CERN-TH.6113/91, WUP 91-23, PSI-PR-91-14 (1991).

[58] E.H. Thorndike (CLEO Collaboration), Contributed paper # 531, LP-HEP 91 Conference, Geneva, Switzerland (1991).

[59] C. Albajar et al. (UA1), CERN Report-PPE/91-55(1991).

[60] A.J. Buras and P.H. Weisz, Nucl. Phys. **B333** (1990) 66;
A.J. Buras et al., MPI-Muñchen Report, MPI-PAE/PTh 56/91 (1991).

[61] B.A. Campbell and P.J.O'Donnell, Phys. Rev. **D25** (1982) 25.